Computers and Chemical Engineering 194 (2025) 108955

Contents lists available at ScienceDirect

Computers and Chemical Engineering

journal homepage: www.elsevier.com/locate/cace

Optimization-based process synthesis by phenomena-based building blocks and an MINLP framework featuring structural screening

David Krone [a,*], Erik Esche [a,c], Mirko Skiborowski [b], Jens-Uwe Repke [a]

[a] Process Dynamics and Operations Group, Technische Universität Berlin, Straße des 17. Juni 135, 10623, Berlin, Germany
[b] Institute for Process Systems Engineering, Hamburg University of Technology, Am Schwarzenberg-Campus 4, 21073, Hamburg, Germany
[c] Bundesanstalt für Materialforschung und -prüfung (BAM), Unter den Eichen 87, 12205, Berlin, Germany

ARTICLE INFO

Keywords:
Process synthesis
Superstructure optimization
Distillation
Mathematical programming
Structural screening

ABSTRACT

An existing approach for optimization-based process synthesis with abstracted phenomena-based building blocks (PBB) is extended by implementing it into a novel MINLP framework with structural screening. Consistency across the multilayer MINLP framework is guaranteed by creating a MathML/XML data model and subsequently exporting the code to the different program parts. The novel framework focuses both on fidelity by implementing thermodynamically sound models and on generality by employing a state-space superstructure that spans a large search space. In order to retain tractability, we insert a structural screening layer which pre-screens based on binary decision variables of the superstructure by graph- and rule-based analyses, penalizing non-physical instances without solution of the underlying MINLP. The MINLP framework is successfully applied on two challenging synthesis tasks to determine the separation of the feed streams of benzene and toluene, as well as of n-pentane, n-hexane, and n-heptane utilizing superstructures with two, respectively four PBB.

1. Introduction

Notable advancements in energy efficiency have been made within the chemical industry over the past few decades. For instance, the EU's chemical industry experienced an 85% increase in production volume while reducing total energy consumption by 26% between 1990 and 2015 (Kiss and Smith, 2020). However, despite these improvements, the sector continues to be one of the largest energy consumers and greenhouse gas emitters in both the US and EU. In fact, thermal separation processes alone accounted for nearly an eighth of the total energy consumption in the US in 2016 (Sholl and Lively, 2016). Given the current energy crisis and the imperative to achieve carbon neutrality, it is vital to transition to renewable energy sources and significantly reduce energy consumption. This can be achieved through the utilization of, e.g., new reaction pathways, innovative catalysts (including biocatalysts), solvents, and heat integration on the plant level as well as by advanced integrated equipment. These efforts, alongside other process intensification (PI) measures and the discovery of novel sustainable process configurations, have the potential to bring about disruptive changes in the chemical industry. Specifically, the combination of multiple PI measures across various process levels, including the employment of innovative and yet-to-be-discovered equipment, holds promise. According to the classification by Freund and Sundmacher (2011), these different process levels for implementing PI encompass the plant, process unit, phase, and molecular levels. An exemplary highly integrated process that utilizes several PI measures at different levels is the hexanol and butyl acetate transesterification in an enzymatic catalyzed reactive dividing wall column, as described by Egger and Fieg (2017).

However, detecting innovative processes remains a challenge. Chen et al. (2021) emphasize the delicate trade-off between generality, fidelity, and tractability in process synthesis methods. The inclusion of PI options during synthesis further complicates this demanding task. Existing methods often limit the search space by focusing on individual PI options (losing generality) or employing simplified models (losing fidelity).

Several heuristics and databases for PI technologies expand upon established process synthesis methods. Classical systematic generation methods, as the concepts by Douglas (1985) and Smith and Linnhoff (1988), provide step-by-step guidance for designing reaction sections, separation units, energy systems, and utility systems. Although the iterative nature of these methods hampers exploring those PI measures which leverage synergies between different process levels, the heuristics applied at each step can be expanded towards PI, enabling the detection of individual PI technologies. Simplified heuristics and

* Corresponding author.
E-mail addresses: david.krone@tu-berlin.de (D. Krone), erik.esche@tu-berlin.de (E. Esche), mirko.skiborowski@tuhh.de (M. Skiborowski), j.repke@tu-berlin.de (J.-U. Repke).

https://doi.org/10.1016/j.compchemeng.2024.108955
Received 10 February 2024; Received in revised form 15 October 2024; Accepted 26 November 2024
Available online 3 December 2024

guidelines that effectively identify potential applications of specific PI technologies are, e.g., the thermodynamic insight approach introduced by Jaksland et al. (1995) with the extension by Holtbruegge et al. (2014) for reactive or hybrid separations, along with guidelines for energy-intensified distillation (Kiss and Suszwalak, 2012) and reactive distillation (Shah et al., 2012).

Lutze et al. (2012) employ heuristics and adapted databases tailored for PI technologies to reach superior designs starting from a base case in their synthesis method based on evolutionary modification. By implementing multiple algorithms, heuristics, and a large database of different PI technologies, the method advances considerably towards generality. Decomposing unit operations into fundamental phenomena (e.g., reaction, mixing, energy transfer, phase contact, phase change, or phase transition) (Arizmendi-Sánchez and Sharratt, 2008; Lutze et al., 2012), and translating them into equipment addresses the challenge of an ever-growing diverse PI equipment database. This approach is also believed to enable the discovery of new innovative equipment. Being another representative of a method for evolutionary modification, the ProCAFD toolbox for PI (Tula et al., 2020) uses phenomena-based building blocks (PBB) in a three-stage synthesis framework to automatically generate intensified process alternatives. However, both this method and the aforementioned one rely on a base case and a flowsheet simulator, favoring designs close to the base case and requiring engineer-driven model generation and evaluation.

Optimization-based synthesis methods with superstructures overcome these limitations by exploring a broader search space. However, formulating and solving the resulting nonlinear programming (NLP), mixed-integer nonlinear programming (MINLP), or general disjunctive programming (GDP) problems pose challenges. Tractability is a key concern, necessitating the adoption of simplified models to reduce computational complexity at the expense of fidelity.

Two optimization-based synthesis methods, namely the Generalized Modular Framework (GMF) proposed by Papalexandri and Pistikopoulos (1996) and the Abstract Building Blocks (ABB) approach introduced by Demirel et al. (2017), aim to achieve generalized synthesis using abstracted model units. The GMF, which incorporates a versatile heat and mass transfer unit, exhibits practical applications in complex distillation processes, including homogeneous azeotropic and reactive distillation (Ismail et al., 2001), as well as heat-integrated distillation processes (Proios and Pistikopoulos, 2005). By enforcing thermodynamic constraints at the inlet and outlet of the unit, the GMF ensures the validity of the MINLP solution. This simplification contributes to combinatorial compactness, enhancing tractability. Yet, it also results in the absence of temperature and concentration profiles. Nonetheless, the inclusion of orthogonal collocation, as exemplified in ideal systems by Proios and Pistikopoulos (2006) and in non-ideal extractive distillation by Tian and Pistikopoulos (2021), partially addresses this limitation by generating temperature profiles. However, this combined approach necessitates a careful balance between increasing profile accuracy through additional collocation points and potential compromises in tractability.

The ABB approach employs versatile ABB within a 2-dimensional superstructure, showcasing successful applications in heat and mass integration (Li et al., 2018) as well as the synthesis of reactive separations (Demirel et al., 2020). By utilizing global optimization solvers as ANTIGONE, the resulting MINLP problems overcome challenges related to initialization and the inherent large combinatorial complexity. However, when synthesizing more complex process configurations, this approach requires the simplification of the ABB, such as employing techniques like the Fenske–Underwood–Gilliland correlation (Demirel et al., 2019) or specialized iterative solution methods to approximate distillation columns (Demirel et al., 2020). Consequently, the method falls short in the synthesis of complex separation processes and non-ideal systems, as it is unable to utilize the benefits of global optimization.

To address this lack in fidelity of optimization-based synthesis methods, Kuhlmann and Skiborowski (2017) developed the superstructure-based PBB approach. The approach integrates thermodynamically accurate equilibrium-stage models and robust kinetics into a general state-space superstructure. Although the PBB approach sacrifices some of the versatility found in the ABB method, it retains the ability to represent a wide range of PI options. Consequently, the method maintains a high level of generality, as demonstrated by successful applications in the synthesis of a membrane-reactor (Kuhlmann et al., 2019) and membrane-assisted reactive distillation (Kuhlmann et al., 2018). However, solving the MINLP problems associated with the PBB-based superstructure relies on a combination of an evolutionary strategy implemented in Visual Basic for fixing the integer decision variables and optimizing individual instances of the superstructure within Aspen Custom Modeler (ACM). The successful simulation of each instance becomes a prerequisite in the latter step. However, it is important to note that the capabilities of the solvers offered by ACM are limited, necessitating decomposition of larger-scale problems. Both aspects highlight the limited tractability of the approach when dealing with larger problem sizes.

In this contribution, we address the limitations and notable achievements of the PBB approach, particularly its high degree of fidelity, by introducing a novel MINLP framework for optimization-based process synthesis. The proposed framework shares similarities with the aforementioned method and involves integrating abstracted model blocks into a state-space superstructure. Notably, we modify the superstructure compared to the original approach by Kuhlmann and Skiborowski (2017) by including logic constraints in algebraic form to deactivate certain heat exchangers. To enhance the ease of application of the method and its tractable problem size, our contribution focuses on three innovations:

Firstly, unlike in the original method, the resulting MINLP problem is automatically solved without requiring further user interactions. This is achieved by leveraging cutting-edge MINLP and NLP solvers available on a mathematical programming platform, effectively eliminating the reliance on a process simulator and its inherent limitations.

Secondly, we incorporate an intermediate layer for structural screening into our MINLP framework, allowing for the elimination of infeasible or non-physical instances prior to MINLP optimization. While this concept is already present in the PBB approach proposed by Kuhlmann and Skiborowski (2017), our MINLP framework extends the screening process with additional rules and algorithms from network analysis.

Thirdly, our approach is based on a comprehensive problem formulation within a meta model represented in MathML/XML. Leveraging the formulation, we automate the export of the model to executable code for the different program components, including the mathematical programming platform, the external CAPE-OPEN thermo engine, and the platform for structural screening. This is achieved through the utilization of separate User-defined Language Specificators (UDLS) (Tolksdorf et al., 2019) within the web-based modeling and optimization tool MOSAICmodeling, developed at TU Berlin (Merchan et al., 2016). The approach has proven successful in preparing and exporting code for simulations, NLP, and MINLP optimization problems within popular solution frameworks such as Python, MATLAB, GAMS, and AMPL (Esche et al., 2017; Esche, 2015). Notably, it has been applied to tackle complex NLP problems, including one that involves utilizing external CAPE-OPEN thermodynamic models for the separation of a non-ideal system using a dividing-wall column with the support of GAMS (Krone et al., 2022). By adopting this approach, our MINLP framework ensures consistency and promotes an efficient workflow, distinguishing it from other synthesis methods that rely on multiple tools. Notably, a similar effort to streamline the inclusion of multiple tools can be seen in Pyosyn (Chen et al., 2021), an open-source framework for systematic superstructure-based process synthesis that utilizes an object-oriented approach in the programming language

Python. However, Pyosyn has not yet shown successful application for general synthesis problems with rigorous thermodynamics embedded.

After introducing the superstructure model, including the vapor–liquid unit (VL-U) as a specific type of PBB in Section 2 and important deliberations on the combinatorial complexity of the resulting MINLP problems in Section 3, our MINLP solution framework is introduced in Section 4. This includes a detailed introduction of the structural screening layer and rules utilized to eliminate infeasible or non-physical instances. The results of two case studies that illustrate the ability of the novel MINLP framework when applied on two challenging process synthesis tasks to determine the separation trains for the mixture of benzene and toluene, as well as n-pentane, n-hexane, and n-heptane are presented and discussed in Section 5. Finally, Section 6 concludes by summarizing the main contributions of our work and suggests areas for future research.

2. Generic superstructure model

The general superstructure model implemented in the scope of the study, which connects all feed and product streams and all PBB is based on the superstructure model by Kuhlmann and Skiborowski (2017). It consists of a distribution network, feed and product streams, as well as a fixed number of PBB. Two significant extensions are introduced in this publication to increase both the versatility of the superstructure and the accuracy of the optimization results: First, the energy flows for potential pressure alterations and heat exchange inside of the distribution network to meet the phase constraints at the inputs of the attached VL-U are modeled separately. This potentially enables the deactivation of a heat exchanger independent from the activity of the previous pressure device based on logic constraints. Why and how heat exchangers are deactivated is presented in Section 2.4. Second, for a more realistic calculation of the energy flow accompanying a pressure change, the pressure devices and some heat exchangers are moved upstream from their original position inside of the mixer nodes to their new position between the splitter and mixer nodes. A detailed description of the exact positions of the devices and the reasoning behind this alteration is given in Section 2.1.1. These two extensions are implemented exclusively in distribution network DNI, as illustrated in the superstructure shown in Fig. 1. While leading to greater accuracy, the extensions result in significantly larger and thermodynamically, as well as numerically more complex systems, which will be shown by the results of the preliminary case study presented in Section 5.1. Since these systems currently need considerably more time to solve, the recourse to the simplified version of the distribution network DNII, as shown in the superstructure in Fig. 2 is currently suggested for more complex synthesis tasks.

The present study focuses on the development of the MINLP optimization framework. In the initial stage, we concentrate solely on the VL-U as a specific type of PBB (Section 2.2). Note that the exclusive use of this single model block enables the modeling of a variety of distillation processes, which currently constitute the vast majority of separation processes (Sholl and Lively, 2016).

2.1. Distribution network

Both versions of the distribution network share the same structure and logic for distributing streams: they connect N_F feed streams with N_P product streams, and a fixed number of N VL-U. They consist of splitter nodes S_l with $l \in \{1, \dots, 2 \cdot N + N_F\}$, mixer nodes M_k with $k \in \{1, \dots, 2 \cdot N + N_P\}$, and streams that connect each splitter node with each mixer node. All the exit streams of the VL-U assembled in the superstructure as well as the N_F feed streams are connected to a unique splitter node, all input streams of the PBB and the N_P product streams to a unique mixer node. While being generic and able to host all kinds of PBB, the distribution networks in the present study exclusively join VL-U as the only kind of PBB. Since VL-U impose specific thermal constraints on all the streams coming in and out, the nodes are further specified: The two streams exiting a VL-U are in saturated vapor and boiling liquid state, respectively; the corresponding splitter nodes are named accordingly vapor splitters S_l^V ($\forall\, l \in \{1, 3, \dots, 2 \cdot N\text{-}1\}$) and liquid splitters S_l^L ($\forall\, l \in \{2, 4, \dots, 2 \cdot N\}$). In standard mode, phase constraints also guarantee that the streams entering a VL-U are either in saturated vapor or boiling liquid state. Hence, the mixer nodes are named after the thermal state of the exiting stream vapor mixers M_k^V ($\forall\, l \in \{1, 3, \dots, 2 \cdot N\text{-}1\}$) or liquid mixers M_k^L ($\forall\, l \in \{2, 4, \dots, 2 \cdot N\}$). All splitter nodes belonging to feed streams and all mixer nodes belonging to product streams are defined as either vapor or liquid nodes according to the prevailing feed and desired product specifications. Since these specifications may vary depending on the specific separation task, the corresponding superscripts are not yet added in Figs. 1 and 2.

The streams going into the splitter nodes are redistributed to the different mixer nodes by implementing three different sets of binary variables: $\psi^{\text{select}}_{\text{split},l}$, $\psi^{\text{a}}_{\text{split},l,k}$, and $\psi^{\text{b}}_{\text{split},l,k}$. Splitters either redistribute the whole incoming stream $\dot{F}^{\text{in}}_{\text{split},l}$ or split it into a maximum of two substreams (a and b) before redistribution. This is an arbitrary choice to limit the combinatorial complexity of the resulting MINLP to some degree. The flows inside of the distribution network $\dot{F}^{\text{DN}}_{l,k}$ that connect splitter l with mixer k are given by

$$\dot{F}^{\text{DN}}_{l,k} = \dot{F}^{\text{in}}_{\text{split},l} \cdot \left\{ \left(1 - \psi^{\text{select}}_{\text{split},l}\right) \cdot \psi^{\text{a}}_{\text{split},l,k} + \psi^{\text{select}}_{\text{split},l} \cdot \left[\psi^{\text{a}}_{\text{split},l,k} \cdot \xi_{\text{split},l} + \psi^{\text{b}}_{\text{split},l,k} \cdot \left(1 - \xi_{\text{split},l}\right) \right] \right\}. \tag{1}$$

While the following two constraints enforce the existence of exactly one first and second split stream a and b,

$$\sum_{k=1}^{Nk} \psi^{\text{a}}_{\text{split},l,k} = 1 \tag{2}$$

and

$$\sum_{k=1}^{Nk} \psi^{\text{b}}_{\text{split},l,k} = 1, \tag{3}$$

the inequality constraint

$$\psi^{\text{a}}_{\text{split},l,k} + \psi^{\text{b}}_{\text{split},l,k} \leq 1 \tag{4}$$

ensures that these two split streams are in fact redistributed to different mixers. Note that according to (1) the flow of the second split stream will only be greater than 0, if the respective splitter is activated, i.e., $\psi^{\text{select}}_{\text{split},l} = 1$.

In standard mode, constraints at the VL-U input nodes enforce the incoming streams to be in a certain thermal state. The second purpose of the distribution network is, hence, to adapt the pressure and temperature of the streams entering the splitters to the thermal state required at the outlet of the mixers that they are distributed to.

2.1.1. Model equations of distribution network I

As portrayed in Fig. 1, the first version of the distribution network (DNI) realizes the potential change of the thermal state by first adapting the pressure of each substream inside of the network to the level prevailing at the mixer node they are connected to. To avoid expensive compression of vapor streams, streams connecting vapor splitters S_l^V with liquid mixers are condensed before compression by an additional heat exchanger. Subsequently, the streams compressed or expanded to the pressure level prevailing at the mixer node are mixed and heat exchangers inside of the mixer nodes guarantee that the phase constraints imposed by the VL-U input nodes are met. This leads to the following model equations that describe the behavior at the splitter nodes, the stream connections between splitters and mixers, and at the mixer nodes:

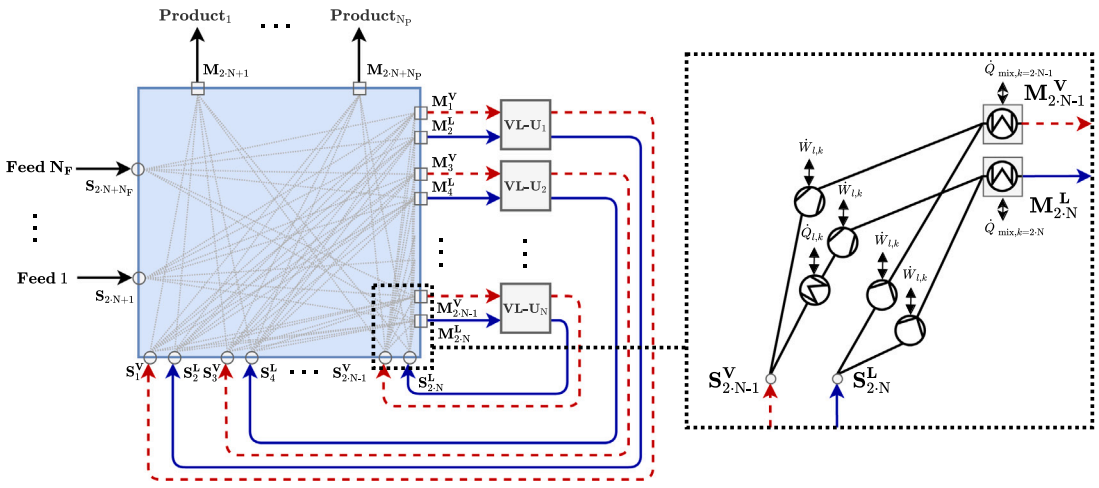

Fig. 1. Schematic representation of a general VL-U-based superstructure based on distribution network DNI (adapted from Kuhlmann and Skiborowski (2017)): it consists of N VL-U, N_F feed streams, N_P product streams, and the corresponding number of mixers (**M**) and splitters (**S**). It includes a detailed depiction of the positions of all potential pressure devices and heat exchangers inside the distribution network as well as at the mixers to meet the phase constraints at each input of the VL-U.

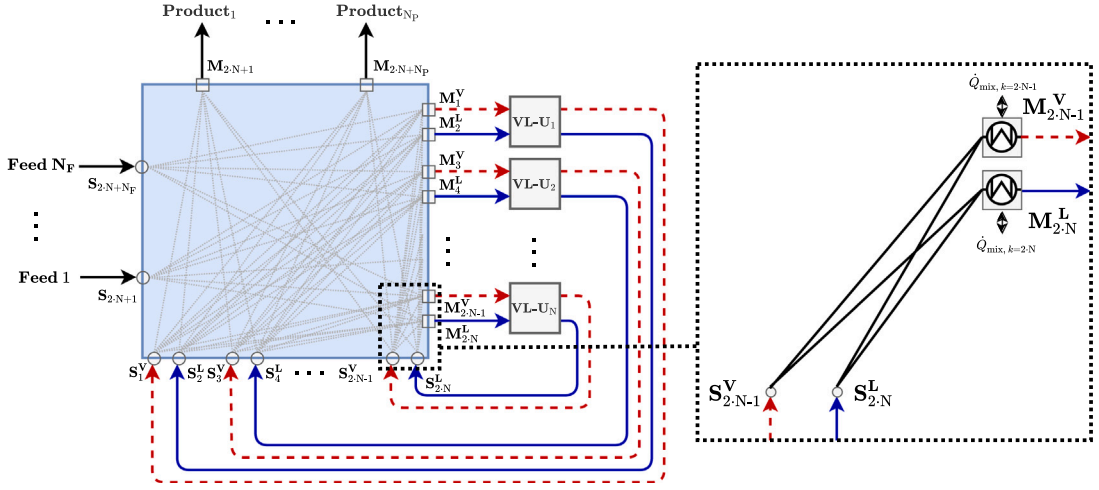

Fig. 2. Schematic representation of a general VL-U-based superstructure based on distribution network DNII (adapted from Kuhlmann and Skiborowski, 2017): it consists of N VL-U, N_F feed streams, N_P product streams, and the corresponding number of mixers (**M**) and splitters (**S**). The heat exchangers to meet the phase constraints at each input of the VL-U are exclusively positioned at the mixers.

DNI – splitters

The substreams leaving a splitter share the molar composition $x^{DN}_{l,k,j}$, specific enthalpy $h^{DN}_{l,k}$, and pressure $p^{DN}_{l,k}$ with the stream entering the respective splitter:

$$x^{DN}_{l,k,j} = x^{in}_{split,l,j}, \tag{5}$$

$$h^{DN}_{l,k} = h^{in}_{split,l}, \tag{6}$$

and

$$p^{DN}_{l,k} = p^{in}_{split,l}. \tag{7}$$

DNI – stream connections from splitters to mixers

Potential alterations of operating pressure between splitter and mixer nodes are modeled via isentropic compression or expansion of the respective connecting stream. The exact position of the pressure devices and the additional heat exchanger for those streams connecting vapor splitters with liquid mixers, as well as all relevant properties are depicted in Fig. 3. To be able to differentiate between the different states within the distribution network, the properties of the streams between the first heat exchanger and the pressure device are referred to by stage 1 (subscript st = 1), whereas all the properties after the pressure devices are referred to by stage 2 (subscript st = 2). The superscript fl marks the **fl**ash properties of both p-s-z and p-T-z flashes, while L and V mark all of the **l**iquid and **v**apor single phase properties.

This results in the following model equations for all the streams $\dot{F}^{DN}_{l,k}$ leaving vapor splitters that are redistributed to liquid mixers, i.e., indexed with $(l,k) \in \{\{1,3,\dots,2\cdot N\text{-}1\},\{2,4,\dots,2\cdot N\}\}$; in addition to the previously introduced variables, the following equations include the specific entropy s, bubble point temperature T^{bub}, flash temperature T^{fl}, and the energy flows of heat exchange $\dot{Q}$ and of pressure alteration $\dot{W}$:

$$\dot{F}^{DN}_{l,k} \cdot h^{DN}_{st=1,l,k} = \dot{F}^{DN}_{l,k} \cdot h^{DN}_{l,k} + \dot{Q}_{l,k}, \tag{8}$$

$$\dot{F}^{DN}_{l,k} \cdot h^{DN}_{st=2,l,k} = \dot{F}^{DN}_{l,k} \cdot h^{DN}_{st=1,l,k} + \dot{W}_{l,k}, \tag{9}$$

$$s^{DN}_{st=2,l,k} = s^{L,DN}_{st=1,l,k}, \tag{10}$$

$$h^{L,DN}_{st=1,l,k} = f\left(x^{DN}_{l,k}, p^{DN}_{l,k}, T^{bub,DN}_{st=1,l,k}\right) \tag{11}$$

$$s^{L,DN}_{st=1,l,k} = f\left(x^{DN}_{l,k}, p^{DN}_{l,k}, T^{bub,DN}_{st=1,l,k}\right) \tag{12}$$

$$T^{bub,DN}_{st=1,l,k} = f\left(x^{DN}_{l,k}, p^{DN}_{l,k}\right), \tag{13}$$

$$h^{fl,DN}_{st=2,l,k} = f\left(x^{DN}_{l,k}, p^{out}_{mix,k}, T^{fl,DN}_{st=2,l,k}\right), \tag{14}$$

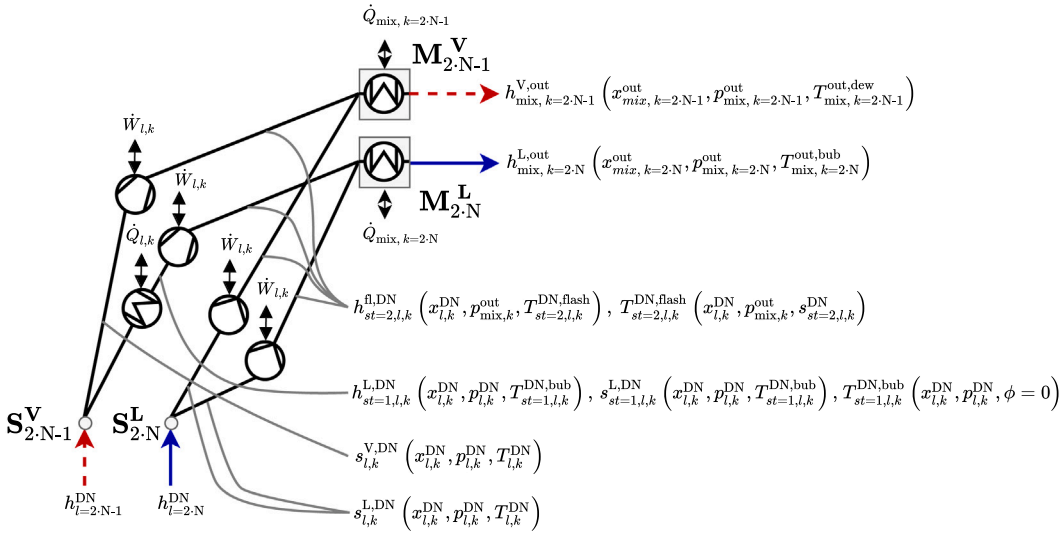

Fig. 3. The four possible stream connections between a splitter and a mixer in DNI (if the heat exchangers are active): the two versions of a splitter — of a vapor stream ($\mathbf{S}^{\mathbf{V}}$) or a liquid stream ($\mathbf{S}^{\mathbf{L}}$) – may connect to the two different versions of a mixer – either designated to forward a vapor ($\mathbf{M}^{\mathbf{V}}$) or a liquid stream ($\mathbf{M}^{\mathbf{L}}$) to a VL-U.

$$T^{\text{fl,DN}}_{st=2,l,k} = f\left(x^{\text{DN}}_{l,k}, p^{\text{out}}_{\text{mix},k}, s^{\text{DN}}_{st=2,l,k}\right), \tag{15}$$
$$\forall\ (l,k) \in \{\{1,3,\ldots,2\cdot\text{N-1}\},\{2,4,\ldots,2\cdot\text{N}\}\}.$$

For all streams $\dot{F}^{\text{DN}}_{l,k}$ leaving liquid splitters and streams leaving vapor splitters that are redistributed to vapor mixers, i.e., indexed with $(l,k),\ l \in \{2,4,\ldots,2\cdot\text{N}\} \cup\ l \in \{1,3,\ldots,2\cdot\text{N-1}\},\ k \in \{1,3,\ldots,2\cdot\text{N}-1\}$, there is no condensation prior to adapting the pressure, hence, the following set of equations is implemented:

$$\dot{F}^{\text{DN}}_{l,k} \cdot h^{\text{DN}}_{st=2,l,k} = \dot{F}^{\text{DN}}_{l,k} \cdot h^{\text{DN}}_{l,k} + \dot{W}_{l,k}, \tag{16}$$
$$s^{\text{DN}}_{st=2,l,k} = s^{\text{L/V,DN}}_{l,k}, \tag{17}$$
$$h^{\text{fl,DN}}_{st=2,l,k} = f\left(x^{\text{DN}}_{l,k}, p^{\text{out}}_{\text{mix},k}, T^{\text{fl,DN}}_{st=2,l,k}\right), \tag{18}$$
$$T^{\text{fl,DN}}_{st=2,l,k} = f\left(x^{\text{DN}}_{l,k}, p^{\text{out}}_{\text{mix},k}, s^{\text{DN}}_{st=2,l,k}\right), \tag{19}$$
$$\forall\ (l,k),\ l \in \{2,4,\ldots,2\cdot\text{N}\}$$
$$\cup\ l \in \{1,3,\ldots,2\cdot\text{N-1}\},\ k \in \{1,3,\ldots,2\cdot\text{N}-1\}$$

Product nodes are defined to always impose a reasonable phase constraint for the respective product. The nodes are then considered as liquid or vapor splitters implying the respective model equations. The same is true for the feed streams, which are set to be in saturated vapor or boiling liquid state.

Note that all properties are calculated via function calls to an external property package. While the first order derivatives of all single phase properties are provided directly by the property package, the derivatives of the flash properties marked by fl are calculated numerically via the finite difference method. These derivatives show a discontinuous jump when reaching states on the bubble point and dew point line. This characteristic is a challenge to most NLP solvers, that rely on consistent derivative information on multiple levels to guarantee convergence and stability, as well as optimality. To eliminate the risk of meeting discontinuities in the solution, a small pressure perturbation of $\Delta p = 0.01$ bar is added to the value of every output pressure $p^{\text{out}}_{\text{mix},k}$. In case of zero pressure change between splitter and mixer node, the state of the stream exiting the pressure device will then lie in the single phase region (for streams from liquid splitters) or in the two-phase region (for streams from vapor splitters), but not exactly on either bubble point or dew point line.

DNI – mixers

Mixing of those streams that are distributed to the same mixer is modeled by the material and energy balances as well as the summation constraint:

$$\dot{F}^{\text{out}}_{\text{mix},k} \cdot x^{\text{out}}_{\text{mix},k,j} = \sum_{l=1}^{\text{Nl}} x^{\text{DN}}_{l,k,j} \cdot \dot{F}^{\text{DN}}_{l,k},\ j = 1,\ldots,(\text{Nc}-1), \tag{20}$$
$$\dot{F}^{\text{out}}_{\text{mix},k} = \sum_{l=1}^{\text{Nl}} \dot{F}^{\text{DN}}_{l,k}, \tag{21}$$
$$\dot{F}^{\text{in}}_{\text{mix},k} \cdot h^{\text{in}}_{\text{mix},k} = \sum_{l=1}^{\text{Nl}} \dot{F}^{\text{DN}}_{l,k} \cdot h^{\text{fl,DN}}_{st=2,l,k}, \tag{22}$$
$$\sum_{j=1}^{\text{Nc}} x^{\text{out}}_{\text{mix},k,j} = 1. \tag{23}$$

Different formulations of the energy balance are implemented for vapor and liquid mixers

$$\dot{F}^{\text{out}}_{\text{mix},k} \cdot h^{\text{V,out}}_{\text{mix},k} = \dot{F}^{\text{in}}_{\text{mix},k} \cdot h^{\text{in}}_{\text{mix},k} + \dot{Q}_{\text{mix},k}, \tag{24}$$
$$\forall\ k \in \{1,3,\ldots,2\cdot\text{N}-1\},$$

$$\dot{F}^{\text{out}}_{\text{mix},k} \cdot h^{\text{L,out}}_{\text{mix},k} = \dot{F}^{\text{in}}_{\text{mix},k} \cdot h^{\text{in}}_{\text{mix},k} + \dot{Q}_{\text{mix},k}, \tag{25}$$
$$\forall\ k \in \{2,4,\ldots,2\cdot\text{N}\},$$

for which the single phase enthalpies of the exiting vapor and liquid streams, $h^{\text{V,out}}_{\text{mix},k}$ and $h^{\text{L,out}}_{\text{mix},k}$, respectively, as well as the corresponding bubble or dew point temperature $T^{\text{dew,out}}_{\text{mix},k}$ and $T^{\text{bub,out}}_{\text{mix},k}$ are determined via the following external function calls:

$$h^{\text{V,out}}_{\text{mix},k} = f\left(x^{\text{out}}_{\text{mix},k}, p^{\text{out}}_{\text{mix},k}, T^{\text{dew,out}}_{\text{mix},k}\right), \tag{26}$$
$$T^{\text{dew,out}}_{\text{mix},k} = f\left(x^{\text{out}}_{\text{mix},k}, p^{\text{out}}_{\text{mix},k}, \Phi=1\right) \tag{27}$$
$$\forall\ k \in \{1,3,\ldots,2\cdot\text{N}-1\},$$
$$h^{\text{L,out}}_{\text{mix},k} = f\left(x^{\text{out}}_{\text{mix},k}, p^{\text{out}}_{\text{mix},k}, T^{\text{bub,out}}_{\text{mix},k}\right), \tag{28}$$
$$T^{\text{bub,out}}_{\text{mix},k} = f\left(x^{\text{out}}_{\text{mix},k}, p^{\text{out}}_{\text{mix},k}, \Phi=0\right) \tag{29}$$
$$\forall\ k \in \{2,4,\ldots,2\cdot\text{N}\}.$$

In (27) and (29), Φ represents the molar vapor fraction of the respective stream.

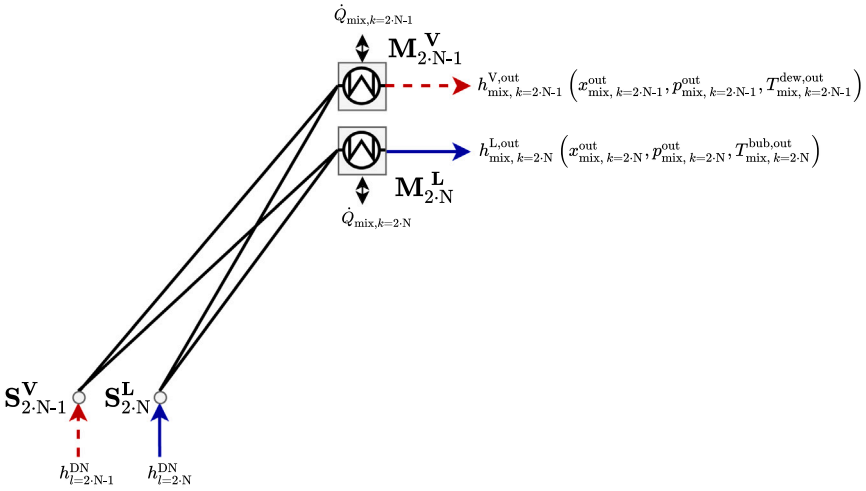

Fig. 4. The four possible stream connections between a splitter and a mixer in DNII (if the heat exchangers are active): the two versions of a splitter — of a vapor stream ($\mathbf{S}^{\mathbf{V}}$) or a liquid stream ($\mathbf{S}^{\mathbf{L}}$) – may connect to the two different versions of a mixer – either designated to forward a vapor ($\mathbf{M}^{\mathbf{V}}$) or a liquid stream ($\mathbf{M}^{\mathbf{L}}$) to a VL-U.

2.1.2. Model equations of distribution network II

The second version of the distribution network (DNII) shown in Fig. 2 does not include any pressure devices. This simplification eliminates any flash property functions that may contain discontinuities in their derivatives. As a result, the system is characterized by a set of functions that are twice continuously differentiable, a prerequisite when solving NLP with state-of-the-art solvers such as IPOPT. However, note that this simplified network can only reasonably be used for synthesis tasks where constant system pressure is assumed across the entire process structure. As depicted in Fig. 4, the thermal states of the streams connecting the splitter with the mixer nodes remain unchanged. So, no further equations are needed for modeling the stream connections between splitter and mixer nodes. As in DNI, the transfer of heat to meet the inlet constraints of the VL-U is confined to within the mixer nodes.

DNII – splitters

DNII shares the splitter Eqs. (5), (6), and (7) with DNI.

DNII – mixers

As in DNI, the single mixed stream subsequently runs through a heat exchanger by which its thermal state is adapted according to the input constraint of the VL-U. Again, the energy flows of the heat exchangers $\dot{Q}_{\mathrm{mix},k}$ are determined by material and energy balances, as well as the summation constraint. DNII shares all the mixer equations with DNI except for Eq. (22), which is adapted to the different variable names:

$$\dot{F}^{\mathrm{in}}_{\mathrm{mix},k} \cdot h^{\mathrm{in}}_{\mathrm{mix},k} = \sum_{l=1}^{\mathrm{Nl}} \dot{F}^{\mathrm{DN}}_{l,k} \cdot h^{\mathrm{DN}}_{l,k}. \tag{30}$$

2.2. VL-U model as a specific type of a PBB

A VL-U, as depicted in Fig. 5, is a counter-current multi-stage contactor of a liquid and a vapor phase. It is based on the VL-PBB introduced by Kuhlmann and Skiborowski (2017) which combines the phenomena mixing of the liquid and vapor phase, phase contacting, energy and mass transfer as well as phase separation. In contrast to the original VL-PBB formulation, reaction as a phenomenon is omitted to simplify the VL-U.

Furthermore, all vapor–liquid equilibria (VLE) are relaxed by adding complementarity constraints (Gopal and Biegler, 1999) to ensure model validity from "all liquid" to "all vapor". The significance of VLE-relaxation for solving complex NLPs with the VL-U as a model unit is shown in several case studies by Krone et al. (2022). The resulting set of model equations for the ith stage of a VL-U is as follows:

$$\dot{F}^{\mathrm{L}}_{i-1} \cdot x_{i-1,j} + \dot{F}^{\mathrm{V}}_{i+1} \cdot y_{i+1,j} = \dot{F}^{\mathrm{L}}_{i} \cdot x_{i,j} + \dot{F}^{\mathrm{V}}_{i} \cdot y_{i,j},\ j = 1,\ldots,\mathrm{Nc}, \tag{31}$$

$$\dot{F}^{\mathrm{L}}_{i-1} \cdot h^{\mathrm{L}}_{i-1} + \dot{F}^{\mathrm{V}}_{i+1} \cdot h^{\mathrm{V}}_{i+1} = \dot{F}^{\mathrm{L}}_{i} \cdot h^{\mathrm{L}}_{i} + \dot{F}^{\mathrm{V}}_{i} \cdot h^{\mathrm{V}}_{i}, \tag{32}$$

$$y_{i,j} = \beta_i \cdot K_{i,j} \cdot x_i,\ j = 1,\ldots,\mathrm{Nc}, \tag{33}$$

$$\sum_{j=1}^{\mathrm{Nc}} x_{i,j} = 1, \tag{34}$$

$$\sum_{j=1}^{\mathrm{Nc}} y_{i,j} = 1, \tag{35}$$

$$h^{\mathrm{L}}_{i} = f\left(x_{i,j}, p^{\mathrm{VL\text{-}U}}, T_i\right), \tag{36}$$

$$h^{\mathrm{V}}_{i} = f\left(y_{i,j}, p^{\mathrm{VL\text{-}U}}, T_i\right), \tag{37}$$

$$K_{i,j} = f\left(x_{i,j}, p^{\mathrm{VL\text{-}U}}, T_i\right), \tag{38}$$

$$\beta_i - 1 = sl^{\mathrm{V}}_{i} - sl^{\mathrm{L}}_{i}, \tag{39}$$

$$\left(sl^{\mathrm{L}}_{i} + t_i\right) \cdot \left(\dot{F}^{\mathrm{L}}_{i} + t_i\right) - \left(t_i\right)^2 \geq 0, \tag{40}$$

$$sl^{\mathrm{L}}_{i} \cdot \dot{F}^{\mathrm{L}}_{i} - \left(t_i\right)^2 \leq 0, \tag{41}$$

$$\left(sl^{\mathrm{V}}_{i} + t_i\right) \cdot \left(\dot{F}^{\mathrm{V}}_{i} + t_i\right) - \left(t_i\right)^2 \geq 0, \tag{42}$$

$$sl^{\mathrm{V}}_{i} \cdot \dot{F}^{\mathrm{V}}_{i} - \left(t_i\right)^2 \leq 0, \tag{43}$$

$$0 \leq x_{i,j}, y_{i,j} \leq 1,\ j = 1,\ldots,\mathrm{Nc}. \tag{44}$$

For a detailed description of the VL-U and all model equations including those added for VLE-relaxation refer to Krone et al. (2022).

2.3. External function calls for CAPE-OPEN thermodynamic properties

All thermodynamic properties, i.e., enthalpies, entropies, equilibrium coefficients, bubble point and dew point temperatures, as well as flash temperatures are implemented as external functions. The functions are formulated as part of the MathML/XML data model and all files needed for the external function calls from GAMS to the CAPE-OPEN external property package via COBIA are generated automatically by code export. For further details on the code export, please refer to Krone et al. (2022).

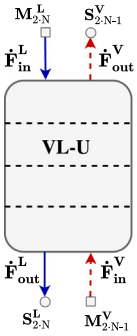

Fig. 5. Schematic representation of the Nth VL-U connected in the superstructure with the respective splitter and mixer nodes of the distribution network with a pair of incoming and outgoing vapor and liquid streams.

2.4. Deactivation of heat exchangers based on logic constraints

In the most general formulation of both versions of the superstructure, the VL-U imposes phase constraints on both inlet streams, i.e., all heat exchangers in the system are always active and all streams leaving the mixers are either in saturated vapor or boiling liquid state, which is why the mixers are given the additional superscript V or L.

Certain combinations of VL-U can be interpreted as a classical distillation column or a sequence of such columns, each equipped with a reboiler at the bottom and a condenser at the top. However, this is only the case if some heat exchangers are deactivated, as, e.g., shown in Fig. 6, where two VL-U are combined by the mixers and splitters of the superstructure. In the given configuration, all the heat exchangers located between the VL-U are deactivated and only those serving as a condenser or reboiler of the column are active. Another configuration with partially deactivated heat exchangers is illustrated in Fig. 7. The structure, which consists of four VL-U, represents a distillation column with a side reboiler and a side condenser for thermal integration within a background process.

For a potential deactivation of the inlet phase constraints as portrayed in the configurations in Figs. 6 and 7, we introduce the binary variable $Y^{\mathrm{HX}}_{\mathrm{mix},k}$:

$$Y^{\mathrm{HX}}_{\mathrm{mix},k} = \begin{cases} 0 & \text{heat exchangers in front of and at mixer } k \\ & \text{are deactivated} \\ 1 & \text{heat exchangers in front of and at mixer } k \\ & \text{stay active.} \end{cases} \tag{45}$$

Next, we adapt the superstructures so that the heat exchangers are only active, if they are interpretable either as a condenser/reboiler of a column or as a side condenser/reboiler, i.e, when an exiting stream is recycled to the inlet of the same VL-U of the opposing phase:

$$\begin{aligned} Y^{\mathrm{HX}}_{\mathrm{mix},k} &= 1 \Leftrightarrow \dot{F}^{\mathrm{DN}}_{l,k} > 0, \\ (l,k) &= \{(1,2),\dots,(2\mathrm{N}-1,2\mathrm{N})\} \\ &\quad \cup\{(2,1),\dots,(2\mathrm{N},2\mathrm{N}-1)\} \end{aligned} \tag{46}$$

and inactive, if there is no such recycle stream:

$$\begin{aligned} Y^{\mathrm{HX}}_{\mathrm{mix},k} &= 0 \Leftrightarrow \dot{F}^{\mathrm{DN}}_{l,k} = 0, \\ (l,k) &= \{(1,2),\dots,(2\mathrm{N}-1,2\mathrm{N})\} \\ &\quad \cup\{(2,1),\dots,(2\mathrm{N},2\mathrm{N}-1)\}. \end{aligned} \tag{47}$$

By implementing the logic relations (46) and (47), it becomes possible to include qualitative terms for the investment costs related to active reboilers and condensers in the objective function. The value of the objective, in turn, will more precisely reflect the total costs of the detected process options.

While the given deactivation logic excludes some energy-efficient structures by, e.g. inhibiting feed preheating or restricting the side reboilers/condensers to reintroduce streams only at the location of their withdrawal, it also has an advantage. Unlike the original superstructure model by Kuhlmann and Skiborowski (2017) that does not deactivate any heat exchangers, the approach identifies designs in which the feed streams are not necessarily fully preheated to saturated vapor. This is significant because, as shown by Bandyopadhyay (2007), excluding feed preheating in favor of side reboilers can result in improved exergetic efficiency in distillation columns.

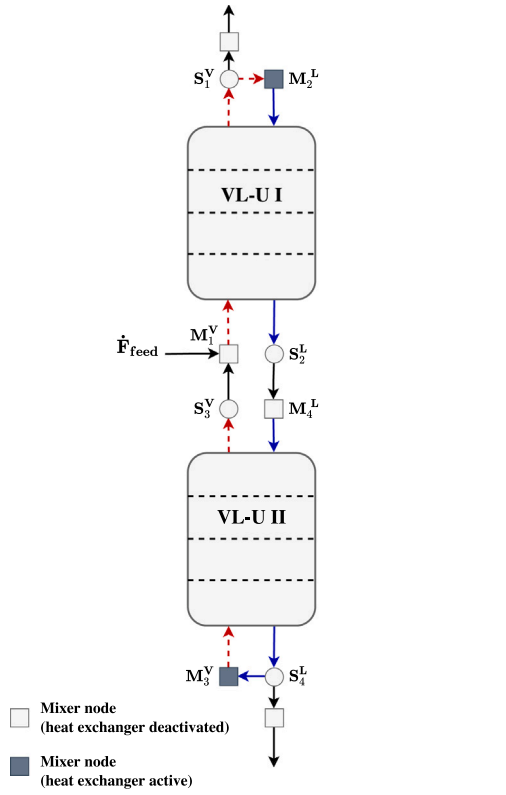

Fig. 6. Schematic representation of a combination of two VL-U interpretable as a column.

Therefore, we introduce the two logic relations (46) and (47) to both versions of the superstructure model. They are reformulated using the big-M method and added to the MINLP:

$$\begin{aligned} & L_1 \cdot \left(1 - Y^{\mathrm{HX}}_{\mathrm{mix},k}\right) + \epsilon_1 \le \dot{F}^{\mathrm{DN}}_{l,k} \\ & (l,k) = \{(1,2),\dots,(2\mathrm{N}-1,2\mathrm{N})\} \\ & \cup\{(2,1),\dots,(2\mathrm{N},2\mathrm{N}-1)\}, \end{aligned} \tag{48}$$

$$\begin{aligned} & \dot{F}^{\mathrm{DN}}_{l,k} \le U_1 \cdot Y^{\mathrm{HX}}_{\mathrm{mix},k} \\ & (l,k) = \{(1,2),\dots,(2\mathrm{N}-1,2\mathrm{N})\} \\ & \cup\{(2,1),\dots,(2\mathrm{N},2\mathrm{N}-1)\}, \end{aligned} \tag{49}$$

with L_1 and U_1 being equal to the lower and upper variable bounds of $\dot{F}^{\mathrm{DN}}_{l,k}$ and $\epsilon_1 = 1 \cdot 10^{-5}$ mol/s.

To fully implement this logic into the two distribution networks DNI and DNII, the constraints implementing the energy balances for heat exchange are adapted and appended by additional constraints. Figs. 8(a) and 8(b) depict all possible connections between splitter and mixer nodes in both distribution networks in the case of deactivated phase constraints. The energy balance of each mixer defined in (24) and (25) for both DNI and DNII is replaced by two separate equality constraints of which only one is activated, while the other one is relaxed and vice versa, depending on the value of $Y^{\mathrm{HX}}_{\mathrm{mix},k}$. This is achieved by introducing the four slack variables $sl^{\mathrm{HX}}_{k,1\text{-}4}$.

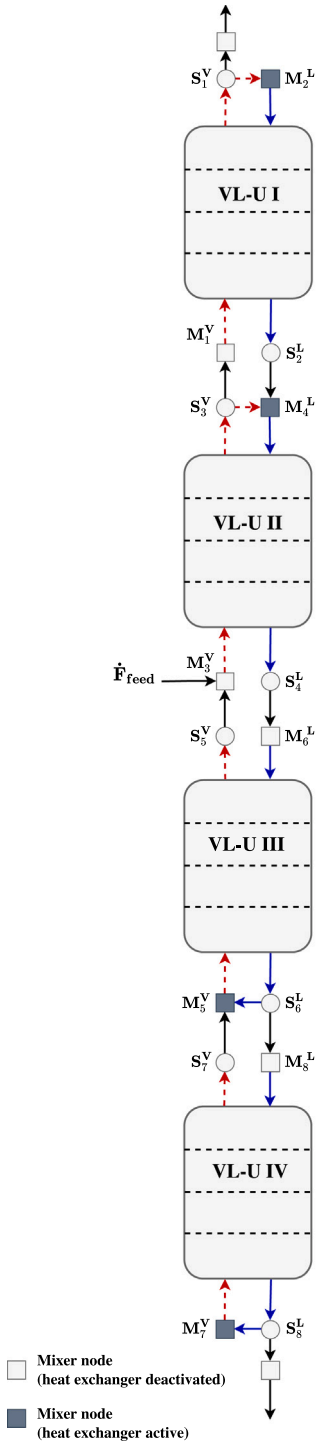

Fig. 7. Schematic representation of a combination of four VL-U interpretable as a column with a side reboiler in the stripping and a side condenser in the rectifying section.

$$\dot{F}^{\text{out}}_{\text{mix},k} \cdot h^{\text{V,out}}_{\text{mix},k} = \left(sl^{\text{HX}}_{k,1} - sl^{\text{HX}}_{k,2}\right) + \dot{F}^{\text{in}}_{\text{mix},k} \cdot h^{\text{in}}_{\text{mix},k} + \dot{Q}_{\text{mix},k}, \tag{50a}$$

$$0 = \left(sl^{\text{HX}}_{k,3} - sl^{\text{HX}}_{k,4}\right) + \dot{Q}_{\text{mix},k}, \quad \forall\, k \in \{1,3,\dots,2\cdot \text{N}-1\}, \tag{50b}$$

$$\dot{F}^{\text{out}}_{\text{mix},k} \cdot h^{\text{L,out}}_{\text{mix},k} = \left(sl^{\text{HX}}_{k,1} - sl^{\text{HX}}_{k,2}\right) + \dot{F}^{\text{in}}_{\text{mix},k} \cdot h^{\text{in}}_{\text{mix},k} + \dot{Q}_{\text{mix},k}, \tag{51a}$$

$$0 = \left(sl^{\text{HX}}_{k,3} - sl^{\text{HX}}_{k,4}\right) + \dot{Q}_{\text{mix},k}, \quad \forall\, k \in \{2,4,\dots,2\cdot \text{N}\}, \tag{51b}$$

$$-U_2 \cdot \left(1 - Y^{\text{HX}}_{\text{mix},k}\right) \le sl^{\text{HX}}_{k,1} - sl^{\text{HX}}_{k,2}, \tag{52}$$

$$sl^{\text{HX}}_{k,1} - sl^{\text{HX}}_{k,2} \le U_2 \cdot \left(1 - Y^{\text{HX}}_{\text{mix},k}\right), \tag{53}$$

$$sl^{\text{HX}}_{k,1} \ge 0, \tag{54}$$

$$sl^{\text{HX}}_{k,2} \ge 0, \tag{55}$$

$$-U_2 \cdot \left(Y^{\text{HX}}_{\text{mix},k}\right) \le sl^{\text{HX}}_{k,3} - sl^{\text{HX}}_{k,4}, \tag{56}$$

$$sl^{\text{HX}}_{k,3} - sl^{\text{HX}}_{k,4} \le U_2 \cdot \left(Y^{\text{HX}}_{\text{mix},k}\right), \tag{57}$$

$$sl^{\text{HX}}_{k,3} \ge 0, \tag{58}$$

$$sl^{\text{HX}}_{k,4} \ge 0, \tag{59}$$

with U_2 being equal to the upper variable bound of the heat flows. The potential bypass of the heat exchanger is completed by adding two more equations and the new variable $h^{\text{out}}_{\text{mix},k}$, which is the specific enthalpy of the stream that is leaving the mixer, whether the heat exchangers are active or not. As before, one of the equations is always relaxed, which is realized by introducing four more slack variables $sl^{\text{HX}}_{k,4\text{-}8}$. This extra step is necessary, because the single phase enthalpies $h^{\text{V, out}}_{\text{mix},k}$ and $h^{\text{L, out}}_{\text{mix},k}$ are implemented as external function calls and always return the enthalpy values for active inlet phase constraints, i.e., in the case of active heat exchangers:

$$\dot{F}^{\text{out}}_{\text{mix},k} \cdot h^{\text{out}}_{\text{mix},k} = \left(sl^{\text{HX}}_{k,5} - sl^{\text{HX}}_{k,6}\right) + \dot{F}^{\text{out}}_{\text{mix},k} \cdot h^{\text{in}}_{\text{mix},k}, \tag{60}$$

$$\dot{F}^{\text{out}}_{\text{mix},k} \cdot h^{\text{out}}_{\text{mix},k} = \left(sl^{\text{HX}}_{k,7} - sl^{\text{HX}}_{k,8}\right) + \dot{F}^{\text{out}}_{\text{mix},k} \cdot h^{\text{V,out}}_{\text{mix},k}, \tag{61}$$

$\forall\, k \in \{1,3,\dots,2\cdot \text{N}-1\}$,

$$\dot{F}^{\text{out}}_{\text{mix},k} \cdot h^{\text{out}}_{\text{mix},k} = \left(sl^{\text{HX}}_{k,7} - sl^{\text{HX}}_{k,8}\right) + \dot{F}^{\text{out}}_{\text{mix},k} \cdot h^{\text{L,out}}_{\text{mix},k}, \tag{62}$$

$\forall\, k \in \{2,4,\dots,2\cdot \text{N}\}$,

$$-U_2 \cdot \left(Y^{\text{HX}}_{\text{mix},k}\right) \le sl^{\text{HX}}_{k,5} - sl^{\text{HX}}_{k,6}, \tag{63}$$

$$sl^{\text{HX}}_{k,5} - sl^{\text{HX}}_{k,6} \le U_2 \cdot \left(Y^{\text{HX}}_{\text{mix},k}\right), \tag{64}$$

$$sl^{\text{HX}}_{k,5} \ge 0, \tag{65}$$

$$sl^{\text{HX}}_{k,6} \ge 0, \tag{66}$$

$$-U_2 \cdot \left(1 - Y^{\text{HX}}_{\text{mix},k}\right) \le sl^{\text{HX}}_{k,7} - sl^{\text{HX}}_{k,8}, \tag{67}$$

$$sl^{\text{HX}}_{k,7} - sl^{\text{HX}}_{k,8} \le U_2 \cdot \left(1 - Y^{\text{HX}}_{\text{mix},k}\right), \tag{68}$$

$$sl^{\text{HX}}_{k,7} \ge 0, \tag{69}$$

$$sl^{\text{HX}}_{k,8} \ge 0. \tag{70}$$

Enabling the potential deactivation of the additional heat exchangers placed in front of the pressure devices in DNI is implemented analogous to the potential deactivation of the heat exchangers at the mixer nodes shown above, i.e., by relaxation of the energy balance (8) and introduction of the alternative constraint, as well as the constraints that determine the enthalpy of the exiting stream. Note that in order to not falsify the optimization results for cases in which, e.g., one

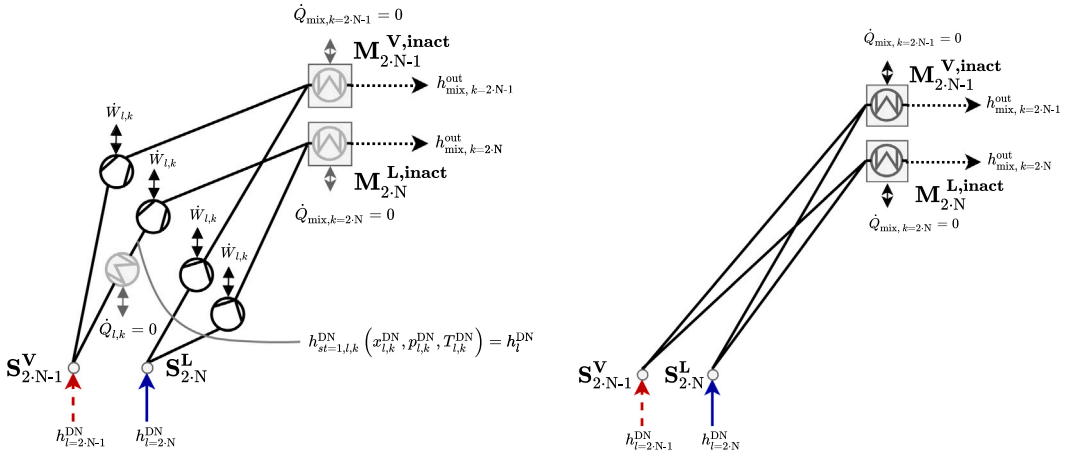

Fig. 8. Schematic representation of the four possible stream connections between a splitter and a mixer in DNI (a) and DNII (b) if the heat exchangers are inactive: the two versions of a splitter – of a vapor stream ($\mathbf{S}^{\mathbf{V}}$) or a liquid stream ($\mathbf{S}^{\mathbf{L}}$) – may connect to the two different versions of a mixer – either designated to forward a vapor ($\mathbf{M}^{\mathbf{V}}$) or a liquid stream ($\mathbf{M}^{\mathbf{L}}$) to a VL-U. The phase constraints are now disabled, hence, all heat exchangers will be deactivated.

or more streams from vapor splitters are connected to a liquid mixer with an inactive heat exchanger, deactivation of the additional heat exchanger is done simultaneously to deactivating the corresponding heat exchanger at the mixer node utilizing the corresponding binary variable $Y^{\mathrm{HX}}_{\mathrm{mix},k}$. In the aforementioned cases, the respective heat of vaporization would otherwise be extinguished for no reason:

$$\dot{F}^{\mathrm{DN}}_{l,k}\cdot h^{\mathrm{DN}}_{st=1,l,k} = \left(sl^{\mathrm{HX}}_{k,9} - sl^{\mathrm{HX}}_{k,10}\right) + \dot{F}^{\mathrm{DN}}_{l,k}\cdot h^{\mathrm{DN}}_{l,k} + \dot{Q}^{\mathrm{V}}_{l,k}, \tag{71a}$$

$$0 = \left(sl^{\mathrm{HX}}_{k,11} - sl^{\mathrm{HX}}_{k,12}\right) + \dot{Q}^{\mathrm{V}}_{l,k}, \tag{71b}$$

$$-U_2\cdot\left(1 - Y^{\mathrm{HX}}_{\mathrm{mix},k}\right) \le sl^{\mathrm{HX}}_{k,9} - sl^{\mathrm{HX}}_{k,10}, \tag{72}$$

$$sl^{\mathrm{HX}}_{k,9} - sl^{\mathrm{HX}}_{k,10} \le U_2\cdot\left(1 - Y^{\mathrm{HX}}_{\mathrm{mix},k}\right), \tag{73}$$

$$sl^{\mathrm{HX}}_{k,9} \ge 0, \tag{74}$$

$$sl^{\mathrm{HX}}_{k,10} \ge 0, \tag{75}$$

$$-U_2\cdot\left(Y^{\mathrm{HX}}_{\mathrm{mix},k}\right) \le sl^{\mathrm{HX}}_{k,11} - sl^{\mathrm{HX}}_{k,12}, \tag{76}$$

$$sl^{\mathrm{HX}}_{k,11} - sl^{\mathrm{HX}}_{k,12} \le U_2\cdot\left(Y^{\mathrm{HX}}_{\mathrm{mix},k}\right), \tag{77}$$

$$sl^{\mathrm{HX}}_{k,11} \ge 0, \tag{78}$$

$$sl^{\mathrm{HX}}_{k,12} \ge 0, \tag{79}$$

$$\dot{F}^{\mathrm{DN}}_{l,k}\cdot h^{\mathrm{DN}}_{st=1,l,k} = \left(sl^{\mathrm{HX}}_{k,13} - sl^{\mathrm{HX}}_{k,14}\right) + \dot{F}^{\mathrm{DN}}_{l,k}\cdot h^{\mathrm{L,DN}}_{st=1,l,k}, \tag{80a}$$

$$\dot{F}^{\mathrm{DN}}_{l,k}\cdot h^{\mathrm{DN}}_{st=1,l,k} = \left(sl^{\mathrm{HX}}_{k,15} - sl^{\mathrm{HX}}_{k,16}\right) + \dot{F}^{\mathrm{DN}}_{l,k}\cdot h^{\mathrm{DN}}_{l,k}, \tag{80b}$$

$$-U_2\cdot\left(Y^{\mathrm{HX}}_{\mathrm{mix},k}\right) \le sl^{\mathrm{HX}}_{k,13} - sl^{\mathrm{HX}}_{k,14}, \tag{81}$$

$$sl^{\mathrm{HX}}_{k,13} - sl^{\mathrm{HX}}_{k,14} \le U_2\cdot\left(Y^{\mathrm{HX}}_{\mathrm{mix},k}\right), \tag{82}$$

$$sl^{\mathrm{HX}}_{k,13} \ge 0, \tag{83}$$

$$sl^{\mathrm{HX}}_{k,14} \ge 0, \tag{84}$$

$$-U_2\cdot\left(1 - Y^{\mathrm{HX}}_{\mathrm{mix},k}\right) \le sl^{\mathrm{HX}}_{k,15} - sl^{\mathrm{HX}}_{k,16}, \tag{85}$$

$$sl^{\mathrm{HX}}_{k,15} - sl^{\mathrm{HX}}_{k,16} \le U_2\cdot\left(1 - Y^{\mathrm{HX}}_{\mathrm{mix},k}\right), \tag{86}$$

$$sl^{\mathrm{HX}}_{k,15} \ge 0, \tag{87}$$

$$sl^{\mathrm{HX}}_{k,16} \ge 0. \tag{88}$$

2.5. Objective function

The objective function Φ to be minimized is a simplified qualitative representation of the annualized costs arising from the resulting process, and it is comprised of three distinct parts: Φ_{InvC} considers the investment costs associated with active heat exchangers, such as reboilers and condensers, Φ_{OpC} represents the operational costs for the heat required by the active reboilers, and the penalty term Φ_{Pen} is included as part of the VLE-relaxation scheme; it vanishes in all solutions of the MINLP.

$$\begin{aligned}&\Phi = \Phi_{\mathrm{InvC}} + \Phi_{\mathrm{OpC}} + \Phi_{\mathrm{Pen}}\\ \Leftrightarrow\ &\Phi = C_{\mathrm{InvC}}\cdot\sum_{k=1}^{2\cdot N}\left(Y^{\mathrm{HX}}_{\mathrm{mix},k}\right)^2 + \\ &C_{\mathrm{OpC}}\cdot\sum_{\substack{k=1,\\ k\in\{1,3,\ldots,2\cdot N-1\}}}^{2\cdot N-1}\left(\dot{Q}_{\mathrm{mix},k}\right)^2 + \sum_{i=1}^{NI}\sum_{n=1}^{N} t_{n,i}\cdot 0\end{aligned} \tag{89}$$

The contributions of investment and operational costs are governed by the constants C_{InvC} and C_{OpC}. The respective values of both constants utilized in the different synthesis tasks are listed in Table 1. Note that the deactivation procedure for inactive heat exchangers as introduced in Section 2.4 enables in the first place to adequately determine the investment cost contributions of the active and, thereby, existent evaporators and condensers in the process structure via binary variables $Y^{\mathrm{HX}}_{\mathrm{mix},k}$. Although the synthesis approach can generate configurations of VL-U that mimic a distillation column, no specific equipment is assumed and as such no accurate investment cost estimates are feasible. As indicated in the work of Kuhlmann and Skiborowski (2017), a more accurate equipment-based process optimization can be conducted after the interpretation of the resulting PBB-configuration

2.6. Initialization

The initialization of MINLP problems is intrinsically challenging, as the structure of the process model is not fixed beforehand and

Table 1
Value of constants C_{InvC} and C_{OpC} in the objective function.

Case study	VL-U [–]	C_{InvC} [€/a]	C_{OpC} [€/(a W^2)]
In Section 5.1	2	10^4	10^{-6}
In Section 5.2	2	10^4	10^{-6}
In Section 5.3	4	10^4	10^{-4}

changes with every iteration based on the current structural binaries. In our method, the system variables are initialized using the results of a successful optimization run on the respective superstructure, employing a constant set of structural binaries. In the case of a superstructure with two VL-U, a configuration interpretable as a column is applied; for a superstructure with four VL-U, a configuration interpretable as a sequence of two columns is utilized. In the first scenario, the minimum product qualities are fixed at 0.95 mol/mol; in the second scenario, they are fixed at 0.70 mol/mol. The initialization of these optimization problems with set structural binaries is done only at a basic level. For example, all flow variables take on the value of the feed stream; temperatures are initialized with the mean value of the boiling points of the high and low boiling components; and all single phase thermodynamic properties, such as enthalpies or entropies, are set to the mean value of the vapor and liquid property of the respective equimolar stream.

3. Scale of combinatorial complexity

The size of the resulting MINLP problem is growing rapidly with the number of PBB that are incorporated into the given superstructure. The maximum number of physically different instances of the superstructure I_{max} that fulfill the three binary constraints (2)–(4) is determined by

$$I_{max} = [2 \cdot N + (2 \cdot N) * (2 \cdot N - 1)]^{N_F} + \left[(2 \cdot N + N_P) + (2 \cdot N + N_P) \cdot (2 \cdot N + N_P - 1)\right]^{2 \cdot N}. \quad (90)$$

E.g., for a superstructure with two VL-U, one feed stream, and two product streams I_{max} is determined at $12.96 \cdot 10^6$ different instances; a superstructure with four VL-U, one feed stream, and three product streams already leads to $4.595 \cdot 10^{16}$ different instances. This illustrates the inherent combinatorial complexity of any practical problem tackled by the given approach. The state-space superstructure provides great generality by spanning a large search space. However, this comes at the inevitable cost of tractability.

In addition to this, the problem size of the MINLP is enlarged by the phase constraint binaries introduced to deactivate heat exchangers and by the variables $t_{n,i}$ utilized for VLE-relaxation. As previously reasoned in Sections 2.4 and 2.5, the phase constraint binaries are considered necessary for achieving interpretable optimization results that do not only represent the operational costs but also reflect relevant contributions to the investment costs of the process structure, i.e., the invest costs for active heat exchangers. Furthermore, considering the difficulties to properly initialize the system that are inherent to superstructure optimization, VLE-relaxation is crucial for solving complex (MI)NLP with multiple VLE, as presented in detail by Krone et al. (2022). The previous aspect is an excellent example for the additional computational costs that entail an increase of fidelity by, e.g., implementing thermodynamically sound equilibrium stages with CAPE-OPEN thermodynamic properties.

4. MINLP framework

The optimization problem resulting from both versions of the superstructure with a fixed number of VL-U is a classical MINLP problem. The problem has got two types of binary decision variables, i.e those that define the connectivity of the VL-U and those that govern the (in-)activity of the inlet phase constraints and, thereby, the heat exchangers, henceforth called structural binaries and phase constraint binaries, respectively. As discussed in Section 3, especially the large quantity of structural binaries needs to be dealt with in order to avoid intractability of the resulting MINLP problems.

Our MINLP framework, as illustrated in Fig. 9, approaches tractability by inserting an intermediate layer of structural screening for the elimination of nonsensical or infeasible instances of the superstructure prior to MINLP optimization. The structural screening procedure, therefore, demands complete insight into the current values of the structural binaries. Since ready-to-use MINLP solvers such as DICOPT or SBB do not supply such insight, a self-written branch-and-bound (B&B) algorithm is implemented as the outer layer of our MINLP framework, to fix an increasingly large set of structural variables to either 0 or 1 (see Section 4.2). Further details on the individual structural screening rules are given in Section 4.4.

A core feature of our MINLP framework that ensures consistency and promotes an efficient workflow is a comprehensive problem formulation within a meta model represented in MathML/XML. Leveraging this formulation, we automate the export of the model to executable code for the different program components, including the mathematical programming platform, the external CAPE-OPEN thermo engine, and the platform for structural screening.

4.1. Code export from MathML / XML data model

As the first step of the MINLP framework, the generic superstructure model in MathML/XML, as well as all files necessary for the structural screening and calling the external CAPE-OPEN property package are exported as an MINLP and included within the specific solution platform. This is achieved through the utilization of separate UDLS (Tolksdorf et al., 2019) within the web-based modeling and optimization tool MOSAICmodeling, developed at TU Berlin (Merchan et al., 2016). The case studies in this publication are all conducted utilizing the modeling and optimization tool GAMS and external property package manager TEA by AmsterChem; the structural screening layer is implemented in MATLAB.

4.2. B&B strategy for insight into values of structural binaries

To retain insight into the current values of the structural binaries, a B&B algorithm is implemented as the outer layer of our MINLP framework. In the outer layer, the structural binaries are gradually fixed to 0 or 1 and the solutions at the different nodes saved or fathomed by standard B&B procedure (step “3. Bounding and Branching”). The full description of the B&B algorithm, which is based on an algorithm by Kalvelagen (2003), is presented in Alg. 1 in the Appendix; the different steps from Fig. 9 reappear in the detailed formulation of the algorithm highlighted, inside a box. After a node is selected (step “1. Node selection”) and prior to be passed on to the MINLP solver (step “2. Optimization of MINLP subproblems”), the MINLP subproblems must successfully undergo the structural screening procedure (“Structural screening”). Activation of any structural screening rule leads to fathoming of the respective node.

4.3. Optimization of MINLP subproblems

Note that the subproblems being forwarded to the solver are MINLP problems, because the phase constraint binaries remain untouched by the outer layer, i.e., are neither fixed nor relaxed by the B&B algorithm. The subproblems are solved in GAMS using DICOPT as MINLP solver, CONOPT as solver for relaxed MINLPs, and IPOPT for NLP subproblems.

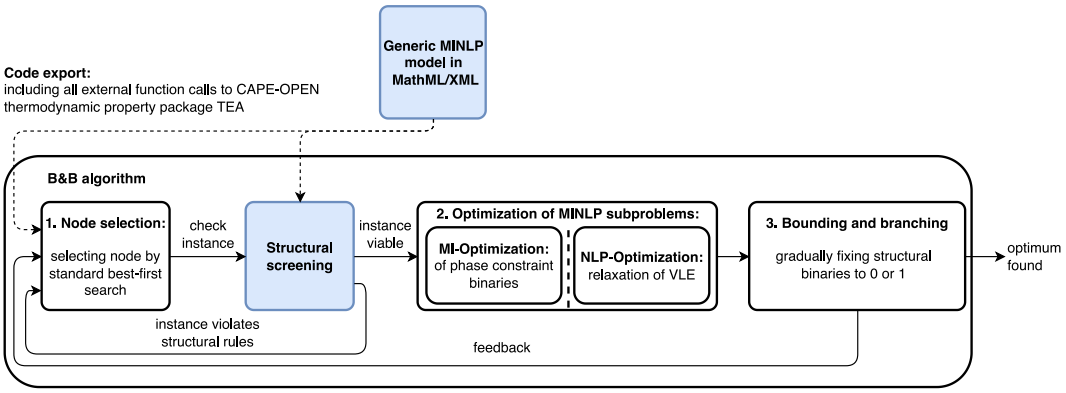

Fig. 9. Structure of the developed MINLP framework with its core features: (1) code export from the generic MINLP model in MathML/XML, (2) the adapted B&B algorithm as the outer layer of the MINLP optimization, as well as (3) an inserted middle layer performing structural screening of the MINLP subproblems.

4.4. Structural screening

The structural screening procedure tests the superstructure instances for both feasibility and sensibility by implementing seven rules, which are divided into the two groups integral screening rules (IR) and functional screening rules (FR). The former impose basic structural requirements, e.g., the fulfillment of the mass balance, while the latter sort out systems that are feasible, but show a lack in functionality, e.g., a system that performs backmixing. The rules sort the systems by checking the current values of the structural binaries both directly and via graph-based methods. To utilize the graph-based methods, the general superstructure is exported as directed graph G to the structural screening layer:

$$G = (V, A), \tag{91}$$

with V being the sum of all nodes in the superstructure (mixer nodes $v_k^{\mathrm{M}} \in V$, splitter nodes $v_l^{\mathrm{S}} \in V$, and nodes $v_n^{\text{VL-U}} \in V$ denoting the location of inlet and outlet streams of the VL-U) and vertices A that represent all existing connections between the nodes. While the connections between the mixer nodes and the VL-U inlet nodes as well as the VL-U outlet nodes and the splitter nodes are always fixed (see Figs. 1 and 2), the vertices between mixer and splitter nodes, i.e., the connections inside of the distribution network, are the result of the concrete values of the structural binaries. The three integral screening rules are:

IR1 *All nodes must have at least one incoming and outgoing stream.* Activation of this rule is shown by the superstructure instances in Figs. 10(a) and 10(b). While the integer constraint (2) enforces that mixer nodes always have at least one outgoing stream, systems with splitter nodes without an inlet stream, as the one shown in Fig. 10(b), may occur and are eliminated, because the VL-U in these systems are dysfunctional. Compliance with this rule is equivalent to:

$$\deg^- \left(v_k^{\mathrm{M}}\right) \geq 1,\ k = 1, \ldots, \mathrm{Nk}, \tag{92}$$

where $\deg^- \left(v_k^{\mathrm{M}}\right)$ denotes the indegree of mixer node $v_k^{\mathrm{M}} \in V$.

IR2 *No isolated cycles/parts in process structure.* Various activations of this rule are shown in Figs. 10(c)–10(e). Compliance with this rule requires the existence of consecutive paths from the feed to each mixer node (including product nodes) as well as, at the same time, from each mixer node (excluding product nodes) to at least one of the product nodes to also eliminate systems as illustrated in Fig. 10(e). Existence of these paths is checked by finding the shortest paths with length d between the above mentioned nodes via the graph algorithm Breadth-first search. A non-existing consecutive path returns path length $d = \inf$.

IR3 *Product streams must be first split streams.* Activation of this rule is shown in Fig. 10(f), where product stream B is the second split stream of the fourth splitter. Note that it is an arbitrary choice to demand product streams to be first and not second split streams. By doing so, however, one eliminates all of the structurally equivalent subproblems, in which product streams are second split streams, before entering the numerically expensive MINLP-optimization. This rule is implemented by checking whether

$$\psi_{\text{split},l,k}^{\mathrm{b}} \cdot \psi_{\text{split},l}^{\text{select}} = 0,\ k = \mathrm{N} + 1, \ldots, \mathrm{N} + \mathrm{N_P}, \tag{93}$$

for all product nodes.

Analogous to the previous integral rule, the following four functional screening rules do not use graph-based methods, but directly check the values of the structural binaries to eliminate the systems that violate any of the given criteria:

FR1 *No nonsensical product stream connections.* Activation of this rule is shown in Figs. 11(a) and 11(b): in the first system, streams from two different splitter nodes are merged into one product node, equivalent to unwanted entropy generation. While we are aware that there are a few valid distillation applications, e.g., multiple effect distillation for sea water desalination, that would be unjustly eliminated by this rule, nonetheless, we decide to apply this rule for our synthesis case studies and suggest to inductively test its implication on the optimization results when applying it to any future synthesis task. In the second system both split streams from one splitter node connect to two different product nodes, which is nonsensical for any purification process.

FR2 *No nonsensical direct recycles (VL-U internally).* Activation of this rule is shown in Figs. 12(a)–12(f). In the first four systems, one of the exiting streams of a VL-U is directly and entirely recycled back to one of its inlets. In the last two systems illustrated in Figs. 12(e) and 12(f) the stream is split and recycled back from the vapor outlet to the vapor inlet or from the liquid outlet to the liquid inlet of the same VL-U. All such direct recycles are considered nonsensical and are eliminated. Note that this rule is not activated if a stream is split and recycled back from the vapor outlet to the liquid inlet or from the liquid outlet to the vapor inlet of the same VL-U, as illustrated in 6.

FR3 *No dysfunctional VL-U.* Activation of this rule is shown in Figs. 13(a) and 13(b). Compliance with this rule requires that the two inlet streams of one VL-U do not originate from the same outlet stream, i.e., the same splitter node.

FR4 *No backmixing of streams.* Activation of this rule is shown in Figs. 14(a)–14(d). Compliance with this rule requires that the two outlet streams of one VL-U are neither directly backmixed by a connection to the same mixer node nor indirectly backmixed by a connection to the two inlets of the same VL-U.

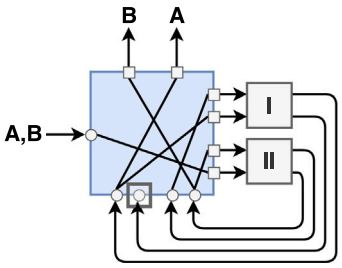

(a) System activating IR1: Splitter node without exit stream.

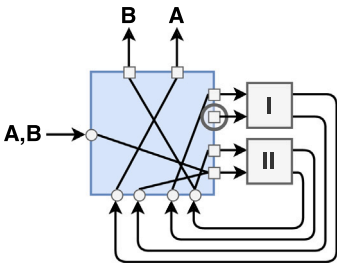

(b) System activating IR1: Mixer node without inlet stream.

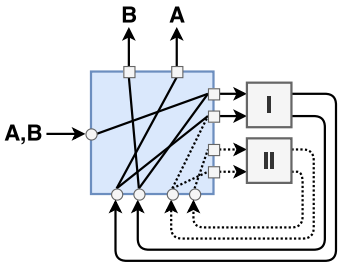

(c) System activating IR2: isolated part in process structure.

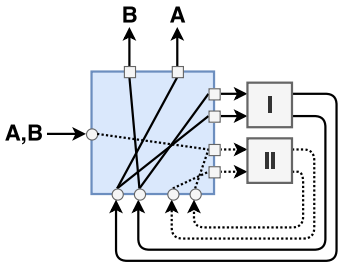

(d) System activating IR2: isolated part in process structure and violation of overall mass balance.

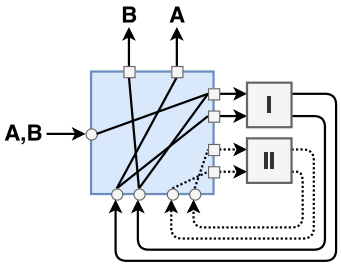

(e) System activating IR2: isolated part in process structure.

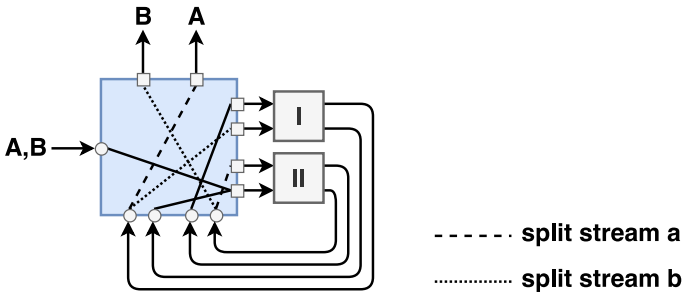

(f) System activating IR3.

Fig. 10. Instances of superstructures with an exemplary number of 2 VL-U that illustrate activating of the three integral rules of the structural screening procedure.

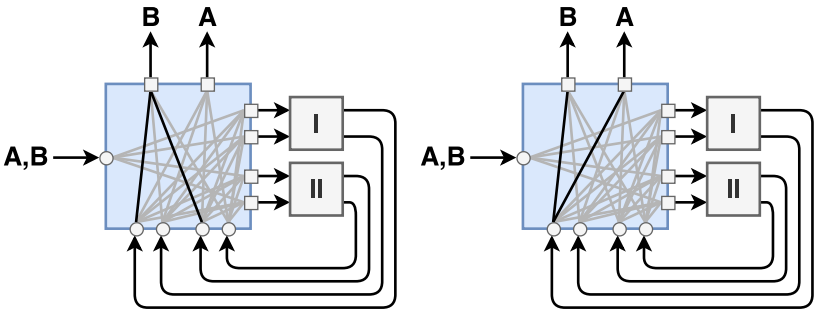

(a) (b)

Fig. 11. Instances of superstructures with an exemplary number of 2 VL-U that illustrate activation of FR1 of the structural screening procedure.

All structural binaries that are previously fixed to either 0 or 1 by the B&B algorithm are considered as such within the screening procedure, whereas those that are relaxed are either cast to a value of 0, or 1, depending on the logic of the specific screening rule, i.e., to 1 for IR1, IR2, and to 0 for IR3, FR1, FR2, FR3, and FR4.

While the concept of structural screening is already present in the PBB approach proposed by Kuhlmann and Skiborowski (2017) and rules IR2 and FR4 and the first part of FR2 (violations shown in Figs. 12(a)–12(d)) enforce criteria published by them, our MINLP framework extends the screening process with additional rules and algorithms from network analysis. All integral rules and part of the formulations of the functional rules FR2 and FR4, i.e., those parts that eliminate instances shown in Figs. 12(a)–12(d), 14(a) and 14(b), are general and hold true for other PBB, while the rest of the rules take into account the special functionality of the VL-U.

Note that the structural screening is implemented out of practicability rather than as an absolute necessity as it is possible but very difficult to enforce the rules as constraints in the original MINLP. This would possibly lead to a heavily "over-constrained" system. However,

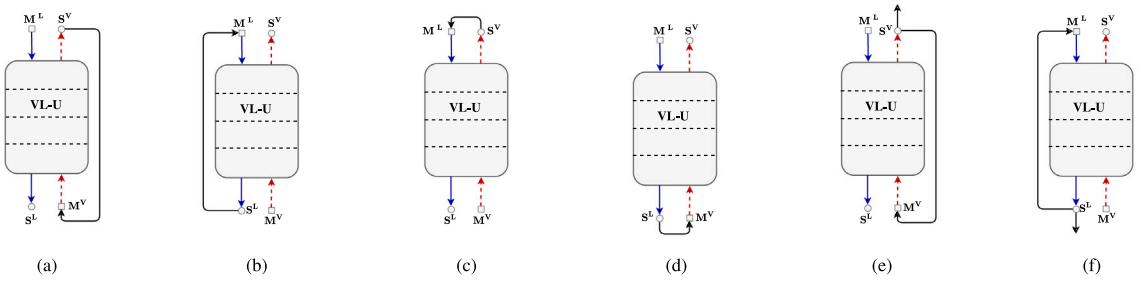

Fig. 12. Instances of superstructures with an exemplary number of 2 VL-U that illustrate activation of FR2 of the structural screening procedure.

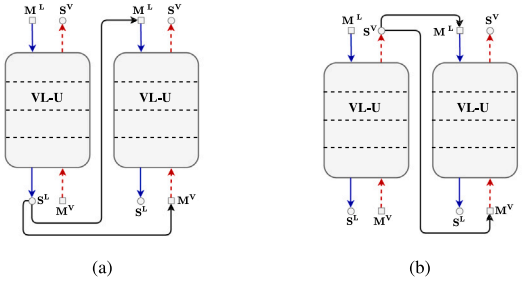

Fig. 13. Instances of superstructures with an exemplary number of 2 VL-U that illustrate activation of FR3 of the structural screening procedure.

with regard to utilizing graph-based methods, the structural screening is without any alternative, since it is yet unknown whether the functionality of graph-based methods – and, e.g., IR2 can only be enforced by a graph-based method –, can even be translated as simple algebraic constraints.

5. Case studies

The following case studies illustrate the ability of our MINLP framework when applied on the process synthesis tasks to determine the separation trains for the mixtures of benzene and toluene as well as n-pentane, n-hexane, and n-heptane. The preliminary study presented in Section 5.1 is included to establish the choice of the simplified distribution network DNII for the subsequent two synthesis case studies presented in Sections 5.2 and 5.3, since it performs considerably better than distribution network DNI. The preliminary study illustrates this by the separation of a feed stream of benzene and toluene via a system of two VL-U with a fixed number of five equilibrium-stages; the structural binaries are fixed as constants to a set that represents the classical column configuration, as illustrated in Fig. 6, but the four phase constraint binaries remain unfixed, hence, still yielding an MINLP problem.

The synthesis tasks are realized by incorporating two, respectively four VL-U with a fixed number of five equilibrium stages into the superstructure. For the first synthesis task (binary mixture), all structural binaries are unfixed, while the second task (ternary mixture) explores the location of the feed inlet and of one VL-U, i.e., VL-UI, in a partially fixed structure. This aims to contain the complexity of the larger system to the already high number of 62 binary decision variables. Table 2, listing the number of VL-U and binary decision variables for each case study, shows that the binaries examined in the second synthesis case study, thereby, already exceed those in the first: 62 versus 60 binary decision variables. Section 5.4 highlights the importance of the structural screening procedure and provides quantitative information on the specific screening rules activated during MINLP optimization performed for both synthesis studies.

The decision to set each VL-U to five equilibrium stages was made arbitrarily, but with careful consideration to maintain the tractability of the resulting MINLP problem. The selection of five stages is considered to be a reasonable number that provides a balance between computational complexity, mainly due to the VLE-relaxation performed on each stage, and the quality of results. This number is increased or replaced by a varying number via inclusion of additional integer variables, once the framework's efficiency has been enhanced by, e.g., improving initialization of the (MI)NLP subproblems.

5.1. Separation of a benzene and toluene mixture by a distillation column configuration

The corresponding instance of the superstructure with fixed stream connections is shown in Fig. 15. The feed stream of 3.6 kmol/h has the equimolar composition $x_{\mathrm{B}}^{\mathrm{F}} = 0.5$ mol/mol and $x_{\mathrm{T}}^{\mathrm{F}} = 0.5$ mol/mol, a temperature of 373.29 K, and a pressure of 100 kPa (1.84 K above dew point temperature, hence, slightly overheated vapor); the system pressure is kept constant at 100 kPa, and the desired product qualities of $x_{\mathrm{B}}^{\mathrm{A}} \geq 0.98$ mol/mol and $x_{\mathrm{T}}^{\mathrm{B}} \geq 0.98$ mol/mol are enforced via separate inequality constraints.

MINLP optimization of the fixed superstructure with DNI and DNII yields the optima $\Phi = 3.239 \cdot 10^4$ €/a after a CPU time of 3221 s for DNI and $\Phi = 3.238 \cdot 10^4$ €/a after a CPU time of 195 s for DNII. The results show the desired deactivation of all heat exchangers at the mixer nodes that do not serve as a condenser or a reboiler. The small difference between the two values of the objective function (the relative difference is approx. 0.03%) is ascribed to the pressure perturbation Δp added to every output pressure $p_{\mathrm{mix},k}^{\mathrm{out}}$ in DNI. This is done to avoid discontinuities found in the first order derivatives of the flash properties incorporated exclusively in DNI, when reaching states on the bubble point or dew point line in the solution.

However, despite this numeric intervention, there is an obvious deficit in performance of DNI, characterized by the higher CPU time, which is a direct result of the numeric difficulties caused by the above-mentioned discontinuities in intermediate iterates during the solution process. The NLP solvers in use, CONOPT and IPOPT, rely on consistent derivative information on multiple levels to guarantee convergence and stability, as well as optimality. They are, therefore, challenged by functions that are not twice continuously differentiable. A potential solution to this issue is presented by Watson et al. (2017), who use advances in exact sensitivity analysis to overcome the differentiability gaps of flash functions by utilizing generalized derivative information.

Incorporating algorithmic support for generalized derivatives into our MINLP optimization framework extends beyond the intended scope of the discussion of this study. Therefore, we have opted for the simplified DNII model as the distribution network in the subsequent two synthesis case studies. Given that we are working under the assumption of constant pressure throughout the entire system in these two synthesis tasks, DNII, which is a system without pressure devices, can be used without loss of accuracy.

Table 2
Properties of the MINLP problems in the case studies, including the number of VL-U, of structural binaries, of total binaries including those for the phase constraints, of continuous decision variables, and of (in-)equalities.

Case study	No. of VL-U [–]	No. of binaries		No. of continuous decision variables [–]	No. of (in-)equalities [–]
		structural [–]	total [–]		
In Section 5.1	2	0	4	396	504
In Section 5.2	2	56	60	396	504
In Section 5.3	4	54	62	1123	1303

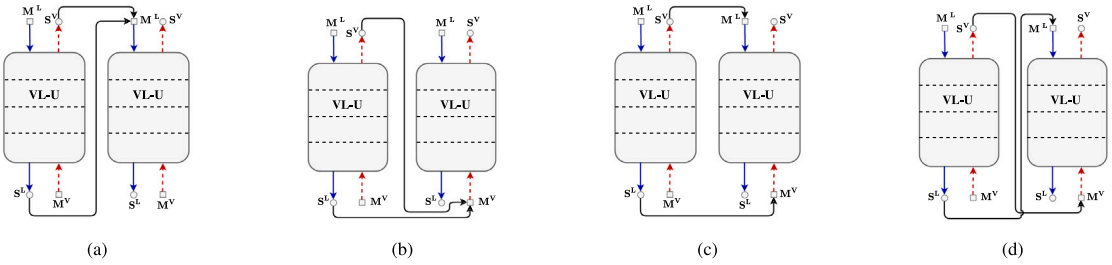

Fig. 14. Instances of superstructures with an exemplary number of 2 VL-U that illustrate activation of FR4 of the structural screening procedure.

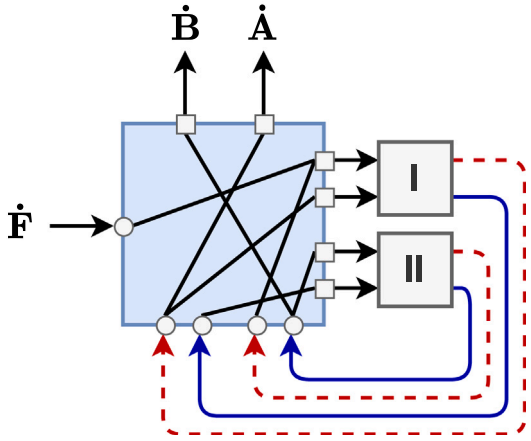

Fig. 15. Superstructure with a fixed set of structural binaries representing a classical column configuration.

5.2. Separation of a benzene and toluene mixture

The first synthesis task is the separation of a feed stream of benzene and toluene by two VL-U with a fixed number of five equilibrium stages. Therefore, two VL-U are incorporated in the superstructure with distribution network DNII; unlike the preliminary study, all stream connections within the superstructure are left unfixed, yielding an MINLP problem with a total of 504 (in-)equalities, 60 binary, and 396 continuous decision variables, as listed in Table 2. The system pressure and desired product qualities are the same as those in the preliminary study. The feed stream properties are changed slightly: it is a stream of 3.6 kmol/h that has the equimolar composition $x^{\mathrm{F}}_{\mathrm{B}} = 0.5$ mol/mol and $x^{\mathrm{F}}_{\mathrm{T}} = 0.5$ mol/mol, a temperature of 370.91 K, and a pressure of 100 kPa, corresponding to a molar vapor fraction of 0.91 mol/mol.

The results of the MINLP optimization are illustrated in Figs. 16(a) and 16(b): the optimal structure interpretable as a distillation column. This finding aligns with the expectations in the context of the given separation task. The value of the objective function is determined at $\Phi = 3.264 \cdot 10^4$ €/a and a reboiler duty of 112.4 kW after 194 iterations of the B&B algorithm and a CPU time of approx. 30 h. This is still quite computationally expensive, but, considering the large structural complexity of the problem, shows the general feasibility of the overall approach.

We would like to emphasize that the results in all case studies are obtained without any specific or manual initialization of the state variables. Currently, all variables are initialized at the midpoints of their respective intervals. This trivial initialization will cause a large part of the high CPU time necessary to solve this and the subsequent case study. Moreover, the VLE formulation, including the interfacing via the CAPE-OPEN standard, is currently not as efficient as it could be. In future work, we plan to evaluate alternative formulations for external computation to increase the speed of the calculation. Previous research by Kuhlmann et al. (2019, 2018) suggests that significant improvements could be achieved using different formulations.

5.3. Separation of an n-pentane, n-hexane, and n-heptane mixture

The second synthesis task is the separation of a feed stream of n-pentane, n-hexane, and n-heptane by four VL-U with a fixed number of five equilibrium stages. Therefore, four VL-U are incorporated in the superstructure with distribution network DNII; as illustrated in Fig. 17(a), the stream connections of the first two splitters and the feed splitter are left unfixed within the superstructure (dotted gray lines), hence, yielding an MINLP problem with a total of 1303 (in-)equalities, 62 binary, and 1123 continuous decision variables, as listed in Table 2. As previously explained, the synthesis task explores the location of the feed inlet and of one VL-U, i.e., VL-UI, in a partially fixed structure, aiming to contain the complexity of the already large system.

The system pressure is again constant at 100 kPa and the desired product qualities of $x^{\mathrm{A}}_{\mathrm{Pen}} \geq 0.80$ mol/mol, $x^{\mathrm{B}}_{\mathrm{Hex}} \geq 0.80$ mol/mol, and $x^{\mathrm{C}}_{\mathrm{Hep}} \geq 0.80$ mol/mol are enforced via separate inequality constraints. Additional inequality constraints ensure that all product flows remain above 0.90 kmol/h. The feed stream of 3.6 kmol/h has the equimolar composition $x^{\mathrm{F}}_{\mathrm{Pen}} = 1/3$ mol/mol, $x^{\mathrm{F}}_{\mathrm{Hex}} = 1/3$ mol/mol, and $x^{\mathrm{F}}_{\mathrm{Hep}} = 1/3$ mol/mol, a pressure of 100 kPa, and a temperature of 351.42 K (saturated vapor).

The results of the MINLP optimization are illustrated in Figs. 17(a) and 17(b): the optimal structure is determined as the structure interpretable as a sequence of two distillation columns. The value of the objective function is determined at $\Phi = 5.561 \cdot 10^4$ €/a, resulting in a combined reboiler duty of 16.58 kW (consisting of $\dot{Q}_{\mathrm{mix},k=3}$ and $\dot{Q}_{\mathrm{mix},k=3}$) after 94 iterations of the B&B algorithm and a CPU time of approx. 172 h.

The results only partly align with the expectations in the context of the given separation task: while the resulting structure is interpretable as two sequential columns, the vapor feed is fed to the upper equilibrium stage of the lower section of the column structure by merging

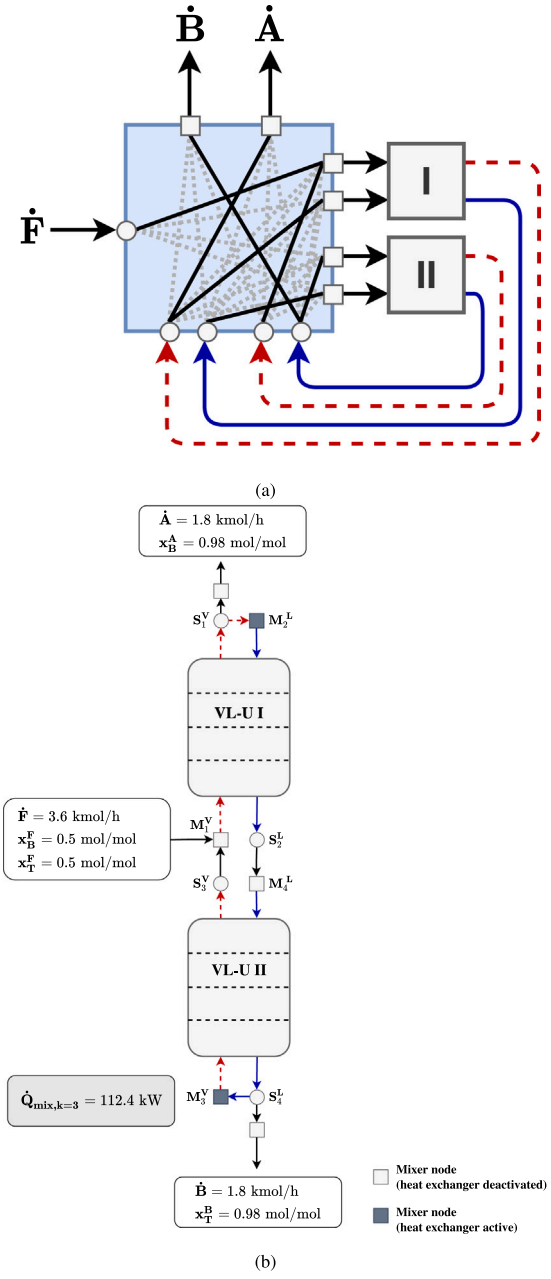

Fig. 16. MINLP optimization results for the separation of a feed stream of benzene, toluene by 2 VL-U: illustrated are the found connections in the superstructure with previously unfixed structural binaries (gray lines) (a) and the result shown in a different view, illustrating the resulting column configuration (b).

it with its liquid inlet stream. This is contrary to the expectation that a saturated vapor feed stream should be added to the vapor inlet of the upper VL-U, as illustrated for the system with fixed structural binaries in Figs. 18(a) and 18(b). The behavior is typically anticipated for columns with a sufficiently large number of stages, which facilitate that the feed is added on a stage where the feed composition equals the one prevailing on the stage, thereby, preventing any loss in efficiency owing to the blending of mixtures with different compositions.

In the given case, however, the column, comprising VL-U I and VL-U II, contains only ten stages, which is insufficient to observe the expected behavior. MINLP optimization of the system with fixed structural binaries as illustrated in 18(a) confirms this, determining a combined reboiler duty of 17.73 kW, which is 6.9% higher than the one determined in the synthesis study. The temperature profiles within VL-U I and VL-U II for the two designs, illustrated in Figs. 19(a) and 19(b), support the finding. The profiles show that the column design determined by the synthesis study (Fig. 19(a)) has fewer losses owing to mixing the feed with the mixture on the feed stage. This can be seen by the greater proximity of the temperatures of the feed and the respective feed stage (stage 5 in 19(a) and stage 6 in 19(b)). Hence, the structure determined by the synthesis study is the optimal structure and the connection of the feed with the liquid inlet of the lower VL-U the result of an "indirect" feed stage optimization performed by the optimizer. "Indirect" as the current structure of the VL-U does not enable feed inlets on stages other than the top or bottom ones.

5.4. Performance of structural screening procedure

The employment of the structural screening procedure is identified as crucial for ensuring the tractability and successful convergence of the MINLP problem as all attempts to solve the MINLP problems without inclusion of the structural screening procedure, i.e., both with our MINLP framework and its outer B&B layer and without it, exclusively utilizing MINLP solvers SBB or DICOPT, render the problem intractable.

During the MINLP optimization for both synthesis tasks, several instances are discarded due to the activation of one or several screening rules: in the first study the screening procedure thereby discards 31 iterates, in the second study 23 iterates, corresponding to 16% respectively 24.5% of the iterations needed by the B&B algorithm to determine the optimal solution. Table 3 lists which of these iterates are discarded due to the activation of one specific rule or a combination of rules. Figs. 20(a) and 20(b) present pie charts that illustrate this distribution. Specifically, the pie charts depict the instances discarded by activation of solely integral rules (dark gray slices), solely functional rules (white slices), and a combination of both rule types (light gray slices).

Interestingly, the mere consideration of feasibility criteria and redundancy via the three integral rules contributes to more than one third of the discarded instances in the respective synthesis study - 11 out of 31 in the first study and 9 out of 23 in the second study. Furthermore, the results add further rationale for the implementation of the various functional rules, which, previously said, are less fundamentally founded than all of the integral rules. However, each of the functional rules is activated multiple times, thereby, considerably reducing the inherent structural complexity of the MINLP problems and contributing to convergence. Therefore, as many functional rules as possible should be defined for each different type of PBB and considered during structural screening. However, this must be done carefully so as not to exclude any promising configurations from the solution space.

6. Conclusions and outlook

In the present contribution, the extension of an existing approach for optimization-based process synthesis with abstracted phenomena-based building blocks is implemented into a novel MINLP framework with structural screening. Consistency is ensured and an efficient workflow of the approach is promoted, by basing it on a comprehensive problem formulation within a meta model represented in MathML/XML, which is exported to executable code for the different program components. The original approach is successfully refined by implementing logic constraints in algebraic form to deactivate certain heat exchangers to achieve interpretable optimization results that also reflect relevant contributions to the investment costs of the process structure, i.e., the invest costs for active heat exchangers. Our MINLP framework is successfully applied on two challenging synthesis tasks to determine the separation of the feed streams of benzene and toluene, as well as of n-pentane, n-hexane, and n-heptane utilizing superstructures with two, respectively four VL-U. The structural screening procedure, which allows for the elimination of infeasible or non-physical instances prior to MINLP optimization, proves crucial for the MINLP to converge

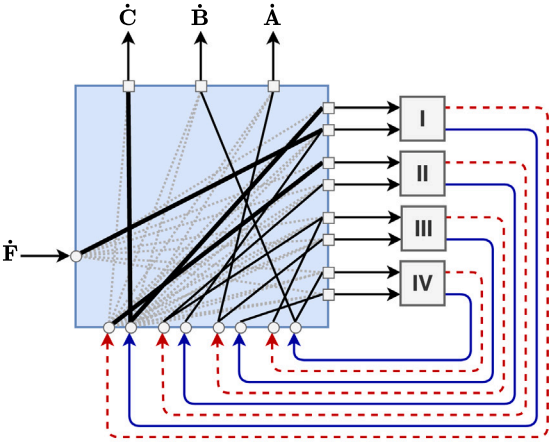

(a)

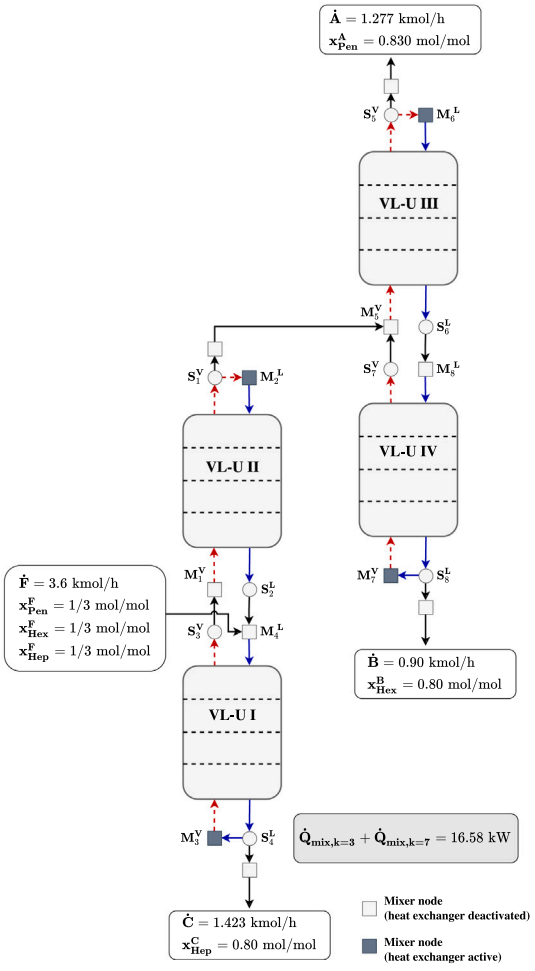

(b)

Fig. 17. MINLP optimization results for the separation of a feed stream of n-pentane, n-hexane, and n-heptane by 4 VL-U: illustrated are the found connections in the superstructure with partially unfixed structural binaries (gray lines) (a) and the result shown in a different view, illustrating the resulting configuration of two sequential columns (b) with feed inlet on the upper stage of VL-UI.

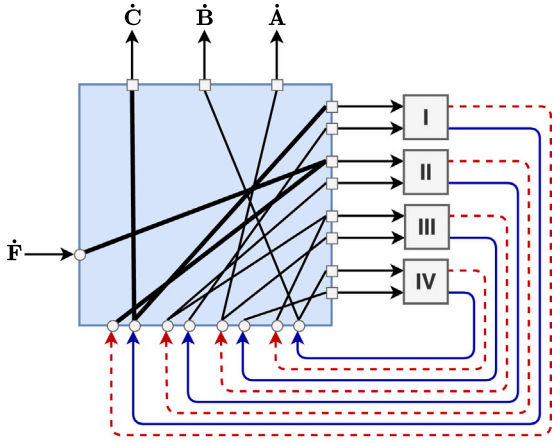

(a)

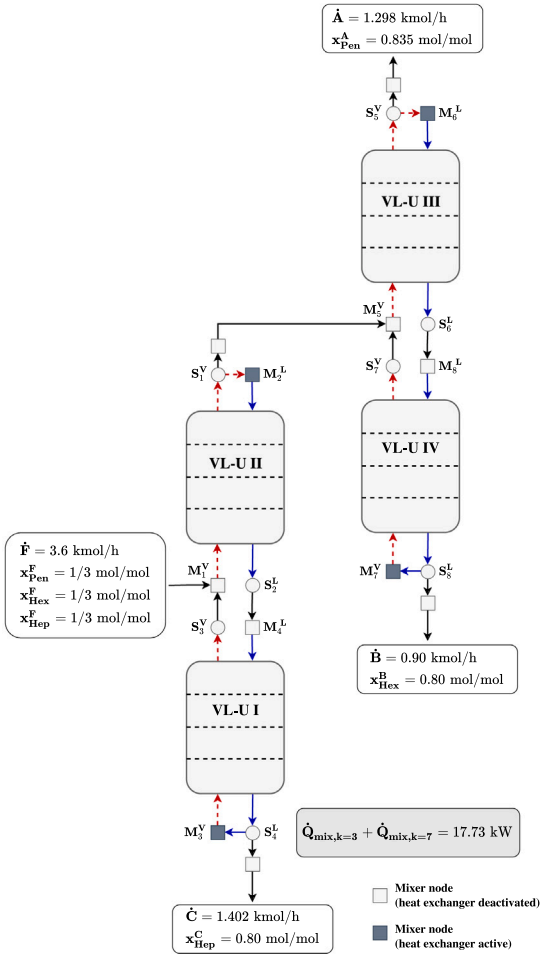

(b)

Fig. 18. Base case for the separation of a feed stream of n-pentane, n-hexane, and n-heptane by 4 VL-U representing 2 sequential columns: connections leading to this design represented in the superstructure (a) and shown in a different view, illustrating the resulting configuration of two sequential columns (b) with feed inlet on the lower stage of VL-UII.

to an optimal structure. All attempts to solve the MINLP problem without structural screening render the problem intractable.

The current work builds the foundation for the development of a general process synthesis tool, which enables the automatic formulation and solution of the highly complex optimization problems, without the need of expert knowledge in optimization, modeling, and problem formulation. The presented framework therefore considerably eases the application of such an approach, while taking care of model fidelity and tractability of the solution. The main advantage in using the MathML/XML-based model formulation lies in flexibility regarding setting up even larger superstructure problems and in flexibility regarding

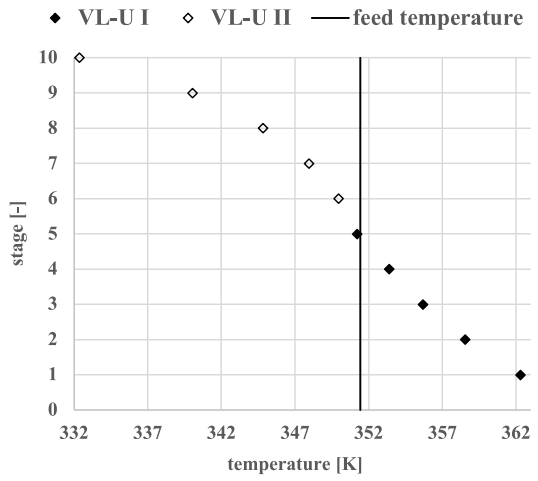

(a)

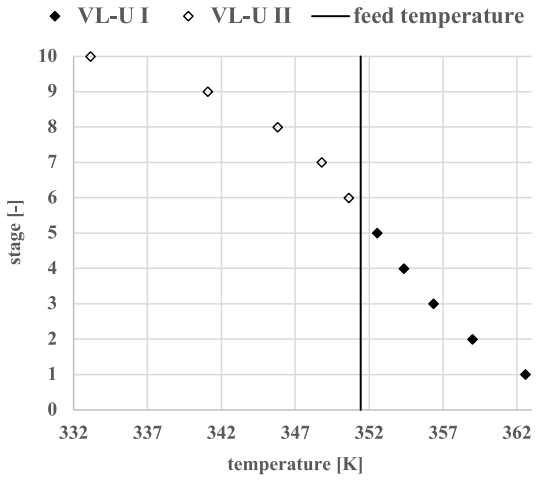

(b)

Fig. 19. Temperature profiles of the n-pentane, n-hexane, and n-heptane mixture within VL-U I and VL-U II during separation by the optimal configuration determined in the case study (feed enters the system on the upper stage of VL-U I) (a), as well as by the reference configuration of two sequential columns, where the feed is added to the vapor stream entering on the lower stage of the upper VL-U (VL-U II) (b). The vertical line in both diagrams indicates the constant temperature of the saturated vapor feed stream at 351.42 K.

the solution environment. A switch from the GAMS/MATLAB/C++ combination to, e.g., a python-based setting should be straightforward.

However, work remains to be done to increase the tractable problem size, thereby extending the applicability of the approach towards a greater number and further types of PBB. Therefore, the continued research focuses on improving the initialization of the (MI)NLP sub-problems by, e.g., utilizing reduced order models and on implementing ideas from generalized disjunctive programming (GDP) for a more compact model formulation with a potentially smaller set of active model equations. Another interesting field for further research is to extend the existing superstructure for heat integration by overlaying it with a second superstructure that performs optimization of internal heat exchange by, e.g., applying the pinch method. Related to this, it is important to address the issue of differentiability gaps within the flash property functions (in DNI) by, e.g., utilizing generalized derivative information to be able to implement all pressure devices as mechanistically correct models.

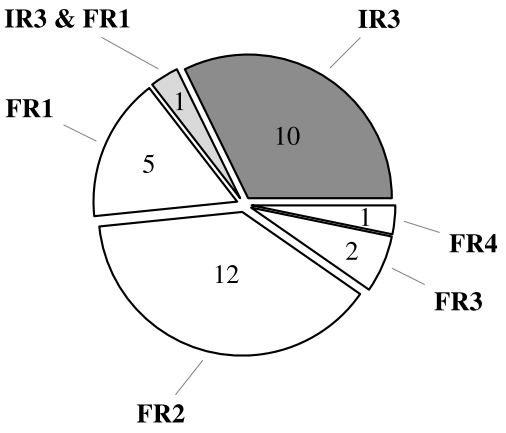

(a)

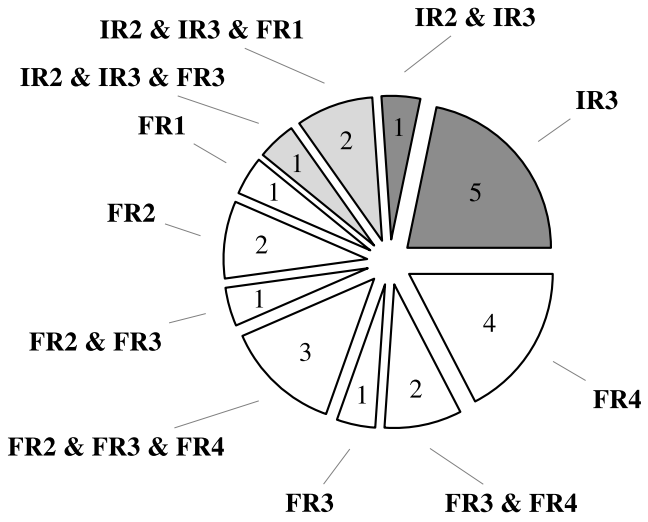

(b)

Fig. 20. Pie charts representing the rules activated during MINLP optimization of the synthesis tasks explored in the case studies in Sections 5.2 (a) and 5.3 (b): The numbers represent the number of iterates at which a specific rule or a combination of them is activated and leads to discarding of a structure.

Table 3
Number of iterates at which a specific rule or a combination of them is activated and leads to discarding of a structure, presented for both synthesis case studies.

Activation of	Synthesis case study in	
	Section 5.2	Section 5.3
IR1	0	0
IR2	0	0
IR3	10	5
FR1	5	1
FR2	12	2
FR3	2	1
FR4	1	4
Simultaneous activation of		
IR2 & IR3	0	1
IR3 & FR1	1	0
IR2 & IR3 & FR1	0	2
IR2 & IR3 & FR3	0	1
FR2 & FR3	0	1
FR2 & FR3 & FR4	0	3
FR3 & FR4	0	2
Iterates with activated rules	31	23

Algorithm 1: B&B algorithm (implemented in GAMS) for solving MINLP synthesis problems resulting from superstructure with several VL-U (based on algorithm by Kalvelagen (2003))

Data: MINLP resulting from generic superstructure of several VL-U
Result: (Optimal) process design
Initialization: Lower (LB) and upper bound (UB) of objective: $LB = 0$, $UB = +\infty$;
Store root node in waiting node list;
while *Waiting node list not empty* **do**
  Node selection – choose a node from the waiting node list by standard best-first strategy (smallest LB of objective first) – equivalent to step "1. Node selection" in Fig. 9;
  if *current network passes structural screening –* "*Structural screening*" *in Fig. 9* **then**
    remove current node from waiting node list;
    solve MINLP of the current node – equals step "2. Optimization of MINLP subproblems" in Fig. 9;
    followed by the subsequent actions summarized by step "3. Bounding and Branching" in Fig. 9;
    if *MINLP is (locally) optimal* ***or*** *feasible but not optimal* **then**
      if *integer solution found* **then**
        if $obj < LB$ **then**
          better integer solution found: $UB = obj$;
          Remove nodes j from waiting node list with $LB_j > UB$;
        else
          fathom current node;
        end
      else
        Variable selection: Find relaxed variable y_k with the value v furthest away from 0 and 1;
        Create two new nodes $j_{new,1}$ and $j_{new,2}$:;
        In $j_{\text{new},1}$: y_k is fixed to 0 (by setting y_k.up = 0);
        In $j_{\text{new},2}$: y_k is fixed to 1 (by setting y_k.lo = 1);
        $LB_{j_{\text{new},1/2}} = obj$;
        Store new nodes $j_{\text{new},1/2}$ in waiting node list;
      end
    else if *MINLP is infeasible* **then**
      fathom current node ;
    else
      solver stopped prematurely for various reasons, e.g., reaching iteration limit;
      Variable selection: Find relaxed variable y_k with value v furthest away from 0 and 1;
      Create two new nodes $j_{new,1}$ and $j_{new,2}$:;
      In $j_{\text{new},1}$: y_k is fixed to 0 (by setting y_k.up = 0);
      In $j_{\text{new},2}$: y_k is fixed to 1 (by setting y_k.lo = 1);
      $LB_{j_{\text{new},1/2}} = +\infty$;
      Store new nodes $j_{\text{new},1/2}$ in waiting node list;
    end
  else
    fathom current node;
  end
end

CRediT authorship contribution statement

David Krone: Writing – original draft, Visualization, Validation, Software, Methodology, Investigation, Formal analysis, Data curation, Conceptualization. **Erik Esche:** Writing – review & editing, Supervision, Project administration, Funding acquisition, Conceptualization. **Mirko Skiborowski:** Writing – review & editing, Conceptualization. **Jens-Uwe Repke:** Writing – review & editing, Supervision, Project administration, Funding acquisition.

Declaration of competing interest

The authors declare that they have no known competing financial interests or personal relationships that could have appeared to influence the work reported in this paper.

Acknowledgments

This work is funded by the Deutsche Forschungsgemeinschaft (DFG, German Research Foundation)–523327609.

Appendix. B&B algorithm

Algorithm shown in Alg. 1.

Data availability

Data will be made available on request.

References

Arizmendi-Sánchez, J.A., Sharratt, P.N., 2008. Phenomena-based modularisation of chemical process models to approach intensive options. Chem. Eng. J. 135 (1–2), 83–94. http://dx.doi.org/10.1016/j.cej.2007.02.017.

Bandyopadhyay, S., 2007. Thermal integration of a distillation column through side-exchangers. Chem. Eng. Res. Des. 85 (1), 155–166. http://dx.doi.org/10.1205/cherd06108R1.

Chen, Q., Liu, Y., Seastream, G., Siirola, J.D., Grossmann, I.E., 2021. Pyosyn: A new framework for conceptual design modeling and optimization. Comput. Chem. Eng. 153, 107414. http://dx.doi.org/10.1016/j.compchemeng.2021.107414.

Demirel, S.E., Li, J., El-Halwagi, M., Hasan, M.M., 2020. Sustainable process intensification using building blocks. ACS Sustain. Chem. Eng. 8 (48), 17664–17679. http://dx.doi.org/10.1021/acssuschemeng.0c04590.

Demirel, S.E., Li, J., Hasan, M.M., 2017. Systematic Proc. Intens. using building blocks. Comput. Chem. Eng. 105, 2–38. http://dx.doi.org/10.1016/j.compchemeng.2017.01.044.

Demirel, S.E., Li, J., Hasan, M.F., 2019. Systematic process intensification. Curr. Opin. Chem. Eng. 25, 108–113. http://dx.doi.org/10.1016/j.coche.2018.12.001.

Douglas, J.M., 1985. A hierarchical decision procedure for process synthesis. AIChE J. 31 (3), 353–362. http://dx.doi.org/10.1002/aic.690310302.

Egger, T., Fieg, G., 2017. Enzymatic catalyzed reactive dividing wall column: Experiments and model validation. AIChE J. 63 (6), 2198–2211. http://dx.doi.org/10.1002/aic.15598.

Esche, E., 2015. MINLP Optimization Under Uncertainty of a Mini Plant for the Oxidative Coupling of Methane (Ph.D. thesis). Technische Universität Berlin, http://dx.doi.org/10.14279/depositonce-4778.

Esche, E., Hoffmann, C., Illner, M., Müller, D., Fillinger, S., Tolksdorf, G., Bonart, H., Wozny, G., Repke, J.-U., 2017. MOSAIC - Enabling large-scale equation-based flow sheet optimization. Chem. Ing. Tech. 89 (5), 620–635. http://dx.doi.org/10.1002/cite.201600114.

Freund, H., Sundmacher, K., 2011. Process intensification, 1. Fundamentals and molecular level. In: Ullmann's Encyclopedia of Industrial Chemistry. John Wiley & Sons, Ltd, http://dx.doi.org/10.1002/14356007.o22_o02.

Gopal, V., Biegler, L.T., 1999. Smoothing methods for complementarity problems in process engineering. AIChE J. 45 (7), 1535–1547. http://dx.doi.org/10.1002/aic.690450715.

Holtbruegge, J., Wierschem, M., Lutze, P., 2014. Synthesis of dimethyl carbonate and propylene glycol in a membrane-assisted reactive distillation process: Pilot-scale experiments, modeling and process analysis. Chem. Eng. Process.: Process. Intensif. http://dx.doi.org/10.1016/j.cep.2014.01.008.

Ismail, S.R., Proios, P., Pistikopoulos, E.N., 2001. Modular synthesis framework for combined separation/reaction systems. AIChE J. 47 (3), 629–649. http://dx.doi.org/10.1002/aic.690470312.

Jaksland, C.A., Gani, R., Lien, K.M., 1995. Separation process design and synthesis based on thermodynamic insights. Chem. Eng. Sci. 50 (3), 511–530. http://dx.doi.org/10.1016/0009-2509(94)00216-E.

Kalvelagen, E., 2003. Branch-and-Bound methods for an MINLP model with semi-continuous variables. URL www.amsterdamoptimization.com/pdf/bb.pdf. (Last Accessed 09 November 2023).

Kiss, A.A., Smith, R., 2020. Rethinking energy use in distillation processes for a more sustainable chemical industry. Energy 203, 117788. http://dx.doi.org/10.1016/j.energy.2020.117788.

Kiss, A.A., Suszwalak, D.-P., 2012. Enhanced bioethanol dehydration by extractive and azeotropic distillation in dividing-wall columns. Sep. Purif. Technol. 86, 70–78. http://dx.doi.org/10.1016/j.seppur.2011.10.022.

Krone, D., Esche, E., Asprion, N., Skiborowski, M., Repke, J.-U., 2022. Enabling optimization of complex distillation configurations in GAMS with CAPE-OPEN thermodynamic models. Comput. Chem. Eng. 157, 107626. http://dx.doi.org/10.1016/j.compchemeng.2021.107626.

Kuhlmann, H., Möller, M., Skiborowski, M., 2019. Analysis of TBA-based ETBE production by means of an optimization-based process-synthesis approach. Chem. Ing. Tech. 91 (3), 336–348. http://dx.doi.org/10.1002/cite.201800119.

Kuhlmann, H., Skiborowski, M., 2017. Optimization-based approach to process synthesis for process intensification: General approach and application to ethanol dehydration. Ind. Eng. Chem. Res. 56 (45), 13461–13481. http://dx.doi.org/10.1021/acs.iecr.7b02226.

Kuhlmann, H., Veith, H., Möller, M., Nguyen, K.-P., Górak, A., Skiborowski, M., 2018. Optimization-based approach to process synthesis for process intensification: Synthesis of reaction-separation processes. Ind. Eng. Chem. Res. 57 (10), 3639–3655. http://dx.doi.org/10.1021/acs.iecr.7b02225.

Li, J., Demirel, S.E., Hasan, M.M., 2018. Process integration using block superstructure. Ind. Eng. Chem. Res. 57 (12), 4377–4398. http://dx.doi.org/10.1021/acs.iecr.7b05180.

Lutze, P., Román-Martinez, A., Woodley, J.M., Gani, R., 2012. A systematic synthesis and design methodology to achieve Proc. Intens. in (bio) chemical processes. Comput. Chem. Eng. 36, 189–207. http://dx.doi.org/10.1016/j.compchemeng.2011.08.005.

Merchan, V.A., Esche, E., Fillinger, S., Tolksdorf, G., Wozny, G., 2016. Computer-aided process and plant development. A review of common software tools and methods and comparison against an integrated collaborative approach. Chem. Ing. Tech. 88 (1–2), 50–69. http://dx.doi.org/10.1002/cite.201500099.

Papalexandri, K.P., Pistikopoulos, E.N., 1996. Generalized modular representation framework for process synthesis. AIChE J. 42 (4), 1010–1032. http://dx.doi.org/10.1002/aic.690420413.

Proios, P., Pistikopoulos, E.N., 2005. Generalized modular framework for the representation and synthesis of complex distillation column sequences. Ind. Eng. Chem. Res. 44 (13), 4656–4675. http://dx.doi.org/10.1021/ie040163m.

Proios, P., Pistikopoulos, E.N., 2006. Hybrid generalized modular/collocation framework for distillation column synthesis. AIChE J. 52 (3), 1038–1056. http://dx.doi.org/10.1002/aic.10711.

Shah, M., Kiss, A.A., Zondervan, E., de Haan, A.B., 2012. A systematic framework for the feasibility and technical evaluation of reactive distillation processes. Chem. Eng. Process. 60, 55–64. http://dx.doi.org/10.1016/j.cep.2012.05.007.

Sholl, D.S., Lively, R.P., 2016. Seven chemical separations to change the world. Nature 532, 435–437. http://dx.doi.org/10.1038/532435a.

Smith, R., Linnhoff, B., 1988. Design of separators in the context of overall processes. Chem. Eng. Res. Des. 66:3.

Tian, Y., Pistikopoulos, E.N., 2021. A Proc. Intens. synthesis framework for the design of extractive separation systems with material selection. J. Adv. Manuf. Process. http://dx.doi.org/10.1002/amp2.10097.

Tolksdorf, G., Esche, E., Wozny, G., Repke, J.-U., 2019. Customized code generation based on user specifications for simulation and optimization. Comput. Chem. Eng. 121, 670–684. http://dx.doi.org/10.1016/j.compchemeng.2018.12.006.

Tula, A.K., Eden, M.R., Gani, R., 2020. Computer-aided process intensification: Challenges, trends and opportunities. AIChE J. 66 (1), http://dx.doi.org/10.1002/aic.16819.

Watson, H.A.J., Vikse, M., Gundersen, T., Barton, P.I., 2017. Reliable flash calculations: Part 2. Process flowsheeting with nonsmooth models and generalized derivatives. Ind. Eng. Chem. Res. 56 (50), 14848–14864. http://dx.doi.org/10.1021/acs.iecr.7b03232.